Semi-Annual Report to NASA Langley for work performed on the grant,

# Flow Structure Generated by Perpendicular Blade Vortex Interaction and Implications for Helicopter Noise Predictions

(NAG-1-1539)

Principal investigators:

William J. Devenport
Aerospace and Ocean Engineering Department,
Virginia Polytechnic Institute and State University,
Blacksburg VA 24061

Stewart A. L. Glegg,
Ocean Engineering Department,
Florida Atlantic University,
Boca Raton, FL 33431

April 1995

# Flow Structure Generated by Perpendicular Blade Vortex Interaction and Implications for Helicopter Noise Predictions

This report summarizes accomplishments and progress on the above project for the period ending April 1995. Much of the work during this period has concentrated on preparation for an analysis of data produced by an extensive wind tunnel test. Time has also been spent further developing an empirical theory to account for the effects of blade-vortex interaction upon the circulation distribution of the vortex and on preliminary measurements aimed at controlling the vortex core size.

## 1. Wind-tunnel test.

Wind-tunnel tests were performed on the idealized configuration shown in figure 1. In this configuration a rectangular NACA 0012 half wing (of aspect ratio 8.65, chord 8") is used to generate a trailing vortex. 15 chordlengths downstream this vortex passes by a simulated helicopter blade. This consists of a similar NACA 0012 wing that spans the entire test section. A full span blade was chosen to eliminate complicating end effects. All measurements were made at a blade chord Reynolds number of 530,000. Boundary layers on both generator and blade were tripped to ensure they were fully turbulent. Full three component velocity, turbulence stress and spectral measurements were made using four-sensor hot-wire probes under computer control. The probes were calibrated directly for flow angle and velocity to ensure the accuracy of the measurements.

The first object of this test was to map out the effects of perpendicular blade vortex interaction as a functions of the most significant independent variables, these being blade vortex separation $\Delta$, streamwise position x, blade angle of attack $\alpha_2$ and vortex strength (controlled by generator angle of attack $\alpha_1$). (Symbols are defined in figures 1 and 2). The second objective was to reveal the flow structure in sufficient depth to enable sound physical explanations (and, if possible, models) of the observed variations to be developed.

The measurements went well and, as can be seen from the enclosed results, the goals were largely achieved. All the tests proposed in the original (two-year) work statement for this project were completed. The measurements we made were also more detailed and extensive than those we originally anticipated in our proposal.

Figures 4 to 23 give a sample of the results. Table 1 shows all the conditions at which measurements were made. The completed test matrix is also illustrated in figures 2 and 3 (solid symbols). Note that each point in the test matrix indicates at least a detailed (80-point) three component velocity and turbulence stress profile of two chordlengths extent measured through the vortex core. In many cases, grids of velocity measurements were also made to document the whole cross-sectional flow structure. Velocity spectra were also measured at the vortex core centers in all cases.

Figures 4 to 8 show the variations of vortex core parameters deduced from these measurements (core radius, circulation, peak tangential velocity and axial deficit) as functions of blade vortex separation, angle of attack and streamwise distance. As can be seen enough points were taken to clearly define the functional variations. Figure 4, for example, shows the core radius and peak tangential velocity as a function of blade vortex separation. The core radius is not

significantly affected for blade vortex separations greater than 1 to 2" (0.125 to 0.25 chords), but is greatly increased below that. The peak tangential velocity at the core edge is more sensitive, there being a significant effect of the interaction for blade vortex separations up to about 3" (0.375 chords). All the effects are very dramatic for low blade vortex separations.

The color figures give a clear picture of some of the physical phenomena behind these variations. The first series (figures 9 to 19) documents the detail the development of the vortex following the interaction in terms of contours of turbulence kinetic energy and mean streamwise vorticity. Initially the blade wake merely cuts the spiral arm of the vortex (figures 9 and 10) and the vortex core appears unaffected. This confirms our conjecture that it is the blade wake that affects the vortex rather than the blade itself. Progressing downstream, the vortex begins to distort and interact with the wake. Most noticeable is the tongue of highly turbulent fluid that forms between the core and wake between x/c=15.95 and 17.5 (figures 11 through 14). This appears to be new turbulence generated by the local instability of the flow here[1] that results from the negative vorticity in the blade wake (figures 10, 12 and 14). This region of turbulence then grows, ultimately engulfing the core and producing a very large region of turbulence surrounding it. (Note the change in scale of the figures as one progresses downstream). The second series (figures 20 through 22), show the effects on the flow at a fixed streamwise location (x/c = 30) of changing the angle of attack of blade and vortex generator together. Most noticeable is the large increase in the scale of the flow and the effects of the interaction with angle of attack.

Note that the data presented here is only a small fraction of that obtained.

2.Study of devices for controlling the vortex core size

The principal task remaining in this project is to determine the influence of vortex core size upon the interaction. A detailed test, with this objective, is planned for May 1995 (see below). A prerequisite of this test is control over the vortex core size. To this end a study has been performed of the effects of various wing-tip modifications on the size of the vortex core shed by the generator wing. Velocity measurements were performed in a small low turbulence wind tunnel (3'x2'x20' test section). The aspect ratio of the wing was reduced to 2.5 so it could be accommodated in this facility. All measurements were made at a location 10 chordlengths downstream of the wing for a chord Reynolds number of approximately 300,000. Many tip modifications (including, rounded tips, full and half end-plates and sub-wings) were found to have small or insignificant effects on the core size. Only one configuration, in which a circular plate was placed at the wing-tip trailing edge perpendicular to the flow, had a large enough influence to be useful for the planned BWI studies. In fact, it was found that by varying the radius of this plate, virtually any desired core size (greater than undisturbed) could be achieved. Vortex cores up to 0.75c diameter were produced. Further details of this study are included in the attached paper. A full report on this study will be completed in early May. It is possible that vortex core diffusers of this type may have practical application on helicopter rotors for reducing parallel BVI noise.

3. Related work on a modified Betz's theory

Perpendicular BVI significantly alters the circulation distribution of the vortex. During the

---

[1]The region of negative streamwise vorticity in the blade wake, when imposed on the vortex results in a non-monotonic circulation distribution which, according to Rayleigh's criterion, should be unstable.

interaction, the velocity field of the vortex changes the circulation distribution on the blade causing the shedding of vorticity. This vorticity (which is both positive and negative) becomes entrained into the vortex, changing its circulation distribution. Significant effort has been spent developing a theoretical model of this process. In this model, a modified form of Prandtl's lifting line theory is used to determine this shed vorticity distribution. This vorticity is then combined with that of the original vortex using an approach similar to Betz's theory. This process is summarized in figure 24. Preliminary comparisons between the theory and data show that the theory overpredicts the quantitative change in circulation distribution during the interaction but qualitatively predicts the nature of the distribution immediately downstream of the blade. We are planning further work working to improve the method and extend it, if possible, to predict the change in vortex core radius during the interaction.

4. Work Related to Helicopter Noise Predictions

The objective of this part of the study is to incorporate helicopter wake codes into the BWI noise prediction scheme and to compare the results with the empirical scheme which was used in earlier studies. Calculations using the CAMRAD wake code have been evaluated and the results are shown in figures 25-27. The case shown is run 649 of the helicopter noise test carried out in the DNW facility in 1986. The advance ratio of the rotor is 0.173 and the tip path plane angle is -3.9°, corresponding to a descent angle of -2.1°. In figure 25 the loci of the vortex interactions with the first following blade are shown. In fig 25 (a) the loci are specified in the rotor plane and the curve marked [1] indicates the first blade vortex interaction. Similarly the curves marked [2] and [3] show the second and third times that the first following blade interacts with the vortex. The interesting point here is that the empirical estimate of the interaction loci gives the same results as the CAMRAD code, which is inherently more accurate. In Figure 25 (b) the vertical displacement of the vortex at the interactions are shown on a scale relative to the blade chord. Only the interaction in the forward arc passes within one chord of the blade, and this result shows a significant difference between the empirical calculations and the CAMRAD calculations. CAMRAD predicts the vortex to pass over the blade whereas the empirical method predicts the vortex to pass underneath the blade. Fortuitously in this case the offset in both cases is the same and since the noise prediction model is based on the offset parameter, similar noise levels would be calculated in either case using this result. However previous studies have shown that it is the second interaction which is more important for BWI noise production and this is illustrated in figure 26. Here again we see that both methods give the same prediction of the interaction location in the rotor plane (Figure 26(a)). In figure 26(b) the vertical scale has been expanded to show all the interactions and in this case better agreement is obtained than for the first following blade. Note that the interaction in the second quadrant of the rotor plane corresponds to the closest interaction (Figure 26(b)) and CAMRAD predicts the vortex to be closer to the blade than the empirical method. This suggests that previous predictions would have been under predicted based on the empirical calculations of blade vortex displacement, and figure 4.4 of the report by Devenport, Glegg, Wittmer and Rife "Perpendicular Blade Vortex Interaction and its implication for Helicopter Noise Prediction" August 1993, indicates that this is the case. Finally Figure 27 shows the third following blade interactions and here it is seen that the empirical method agrees well with CAMRAD. However in this case not only are all the interactions displaced at least one chord from the blade, but they are also almost parallel to the blade leading edge, and not expected to generate BWI noise.

The CAMRAD data was provided in a format which gives the location of the blade tip vortex as a function of wake age for 36 blade locations. Wake age is incremented at intervals of 10° for four revolutions. This spacing is too large to accurately define all the blade vortex interactions in the rotor disc plane, as can be seen by the sparse number of CAMRAD points for the second interaction in Figure 25(a). However it is unnecessary to increase the number of CAMRAD locations for BWI calculations since the interactions which are sparsely calculated are those parallel to the blade leading edge, and not important for BWI. Consequently an interpolation scheme is being developed to provide the information at the locations required for BWI calculations using the CAMRAD data format as provided. This will result in a prediction code which will use CAMRAD data as an input and give BWI noise predictions.

5. Publications

We have produced/are currently producing the following publications;

Kenneth S. Wittmer, William J. Devenport and Stewart A. L. Glegg, 1994, "Perpendicular Blade Vortex Interaction", In press *AIAA Journal.*

Weisser C. M, 1995, "Controlling trailing tip vortices", AIAA 1994 Mid-Atlantic Student Conference, April 21-22, NASA Langley.

K. S. Wittmer and William J. Devenport, 1995, "Interaction of a streamwise vortex with a full span blade", 26th AIAA Fluid Dynamics Conference, June 19-22, San Diego CA. *(abstract accepted)*

6. Plans for the next 6-month period

During the next six months we are planning to complete all the above work and fully document and report it. The major task here will be a second wind tunnel test slated for May. The objectives of this test are (a) to determine the influence of vortex core size upon the interaction. (b) to further document the effects of blade angle of attack and vortex strength upon the interaction. The proposed measurements are shown as the open circles on the test matrix illustrated in figure 3. All measurements will be made at x/c=30, 15 chordlengths downstream of the blade leading edge. Each point in figure 3 represents, at least, a full three-component velocity and turbulence stress profile through the vortex center.

Of highest priority are the measurements to determine the effects of core size. Using the circular plate tip modification developed in the small wind tunnel (see item 2 above), we will use the generator wing produce trailing vortices with core radii 20 and 40%c greater than those studied in the last test. For each core size the effects of the interaction will be investigated for a range of blade vortex separations $\Delta$. Only suction-side interactions (positive $\Delta$) will be examined since these have most relevance to the helicopter problem.

The effects of blade angle of attack will then be examined. Two new blade angles of attack will be used (0 and 10°) giving us data for three in all. For each angle of attack the effects of the interaction as a function of $\Delta$ will be examined. Again only positive $\Delta$'s will be considered. Finally the effects of vortex strength will be examined for constant blade angle of attack (5°) and vortex core size (undisturbed). One new vortex generator angle of attack (10°) will be examined.

As represented in figure 3, the proposed test matrix does not explicitly include examining the effects of combinations of these independent variables (e.g. of increasing the vortex core size and angle of attack together). Measurements of this type are obviously desirable and will be made if any wind tunnel time remains. Some spectral measurements will also be made at selected

conditions to provide further input for the BWI noise prediction method.

| x/c | AOA generator (°) | AOA blade (°) | Δ (") |
|---|---|---|---|
| | | | |
| 30 | 5 | 5 | -4 |
| 30 | 5 | 5 | -3 |
| 30 | 5 | 5 | -2 |
| 30 | 5 | 5 | -1 |
| 30 | 5 | 5 | -0.5 |
| 30 | 5 | 5 | -0.25 |
| 30 | 5 | 5 | 0 |
| 30 | 5 | 5 | 0.5 |
| 30 | 5 | 5 | 0.75 |
| 30 | 5 | 5 | 1 |
| 30 | 5 | 5 | 2 |
| 30 | 5 | 5 | 3 |
| 30 | 5 | 5 | 4 |
| | | | |
| 30 | 2.5 | 2.5 | -1 |
| 30 | 3.75 | 3.75 | -1 |
| 30 | 5 | 5 | -1 |
| 30 | 6.25 | 6.25 | -1 |
| 30 | 7.5 | 7.5 | -1 |
| 30 | 10 | 10 | -1 |
| | | | |
| 30 | 5 | 2.5 | -1 |
| 30 | 5 | 5 | -1 |
| 30 | 5 | 7.5 | -1 |
| | | | |
| 15.16 | 5 | 5 | -1 |
| 15.95 | 5 | 5 | -1 |
| 17.5 | 5 | 5 | -1 |
| 20 | 5 | 5 | -1 |
| 22.5 | 5 | 5 | -1 |
| 25 | 5 | 5 | -1 |
| 30 | 5 | 5 | -1 |
| | | | |
| 15.16 | 5 | 5 | 1 |
| 15.95 | 5 | 5 | 1 |
| 17.5 | 5 | 5 | 1 |
| 20 | 5 | 5 | 1 |
| 22.5 | 5 | 5 | 1 |
| 25 | 5 | 5 | 1 |
| 30 | 5 | 5 | 1 |
| | | | |

**Table 1:** Measurement Conditions

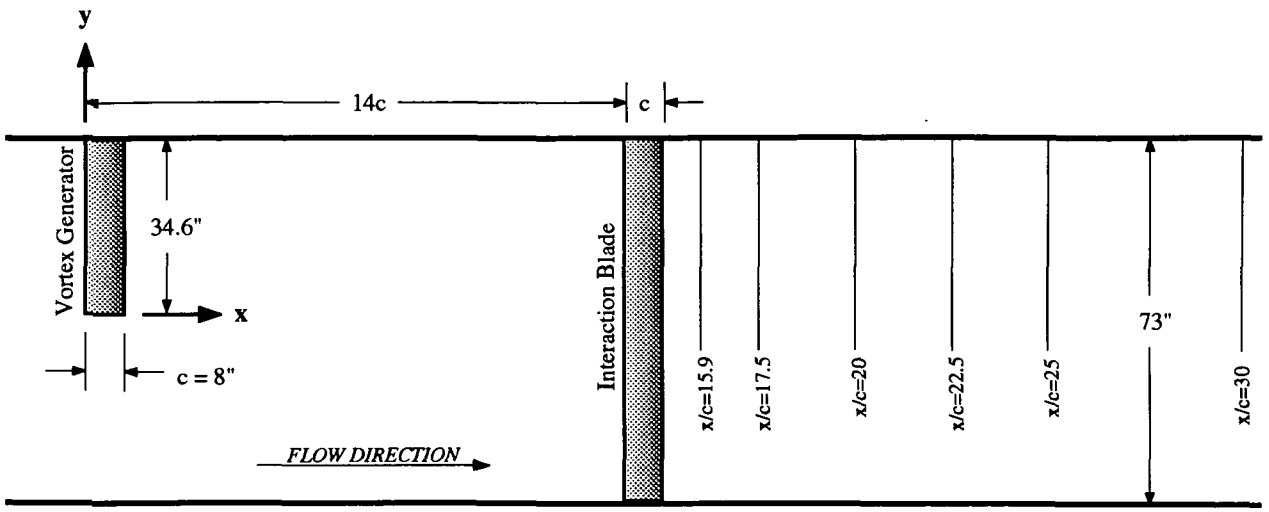


**Figure 1:** Configuration and Coordinate System

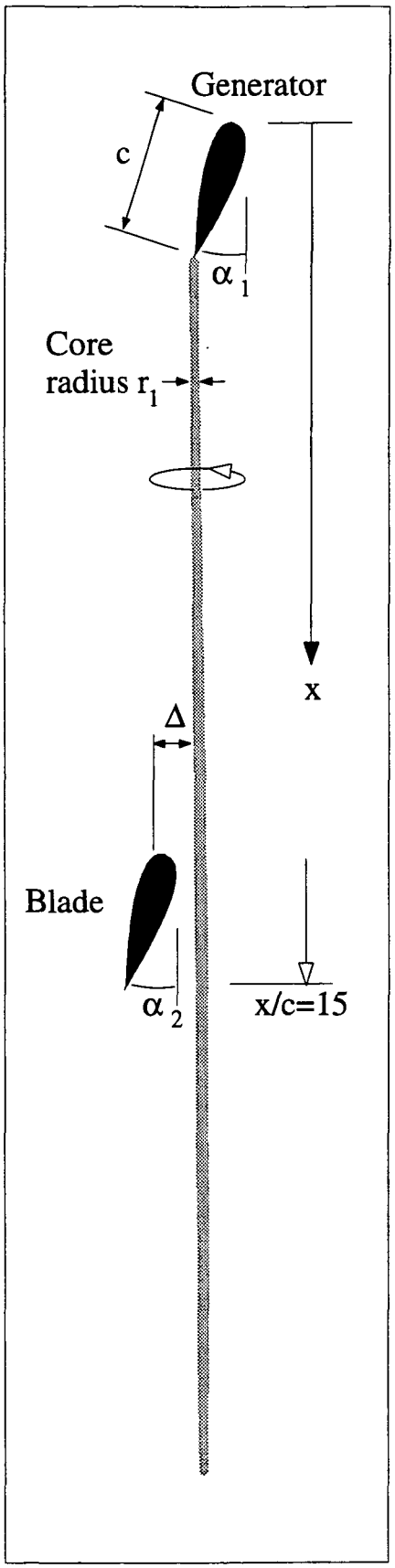


Figure 2. Nomenclature for test matrix in figure 3

**(a) Effect of x/c**

($\alpha_1 = \alpha_2 = 5^o$, $r_1/c = 0.036$)

**(b) Effect of $\alpha_1 = \alpha_2$**

($x/c = 30$, $r_1/c = 0.036$)

**(c) Effect of $\alpha_1$**

($\alpha_2 = 5^o$, $x/c = 30$, $r_1/c = 0.036$)

**(d) Effect of $\alpha_2$**

($\alpha_1 = 5^o$, $x/c = 30$, $r_1/c = 0.036$)

**(e) Effect of $r_1/c$**

($\alpha_1 = \alpha_2 = 5^o$, $x/c = 30$)

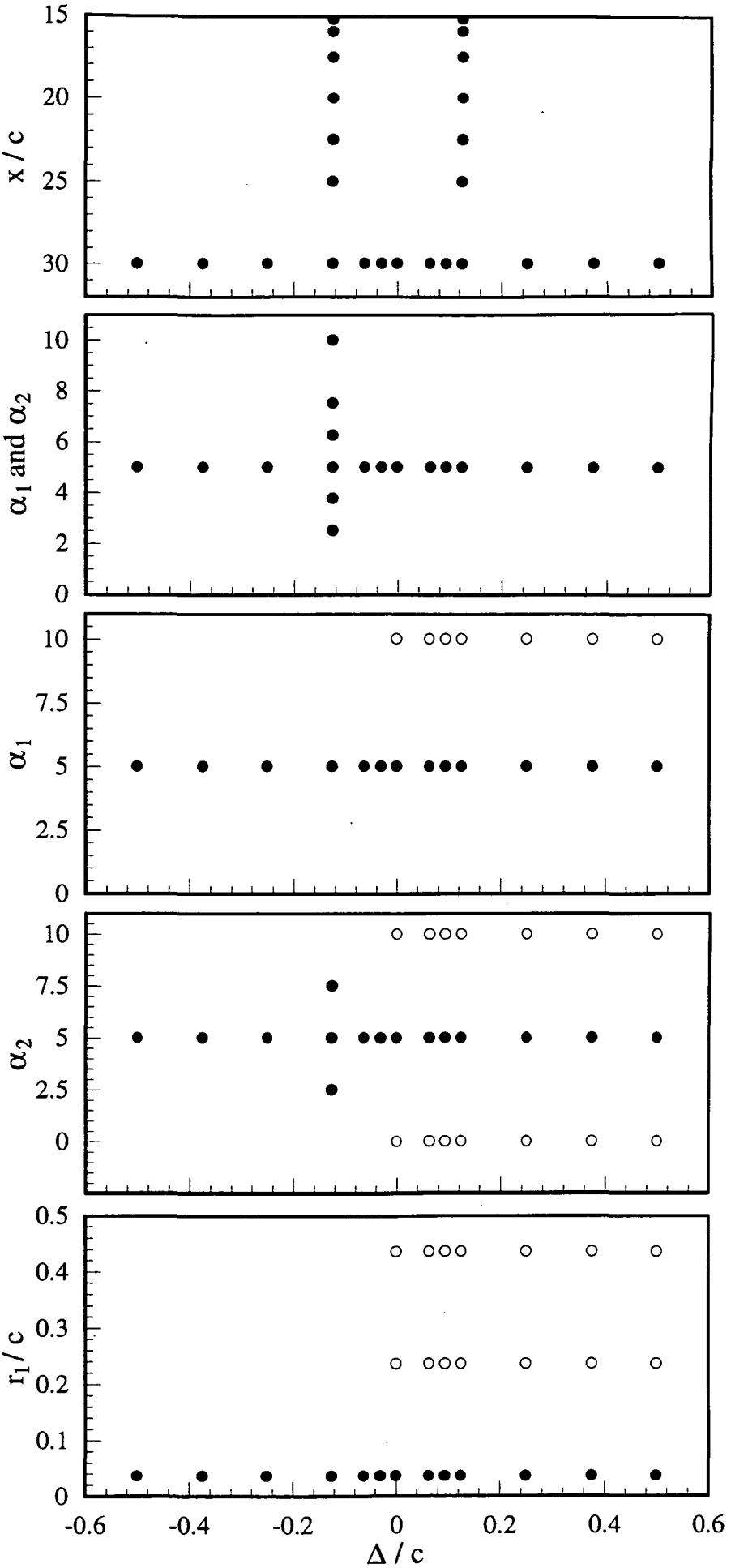


Figure 3. Test matrix. Open circles indicate planned measurements

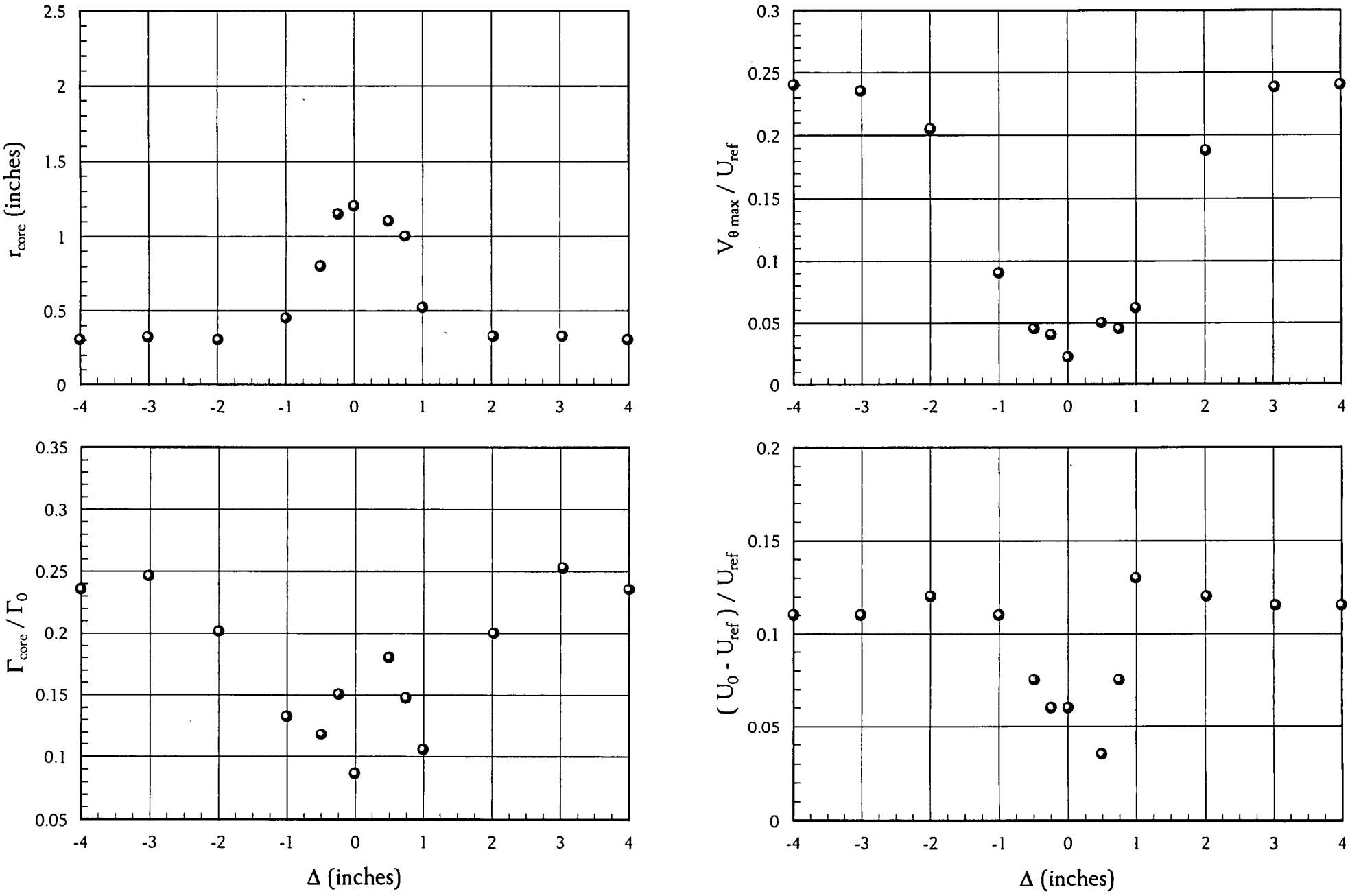


**Figure 4:** Vortex Core Parameters as a Function of Δ at x/c = 30 with Vortex Generator at 5° and Interaction Blade at 5°

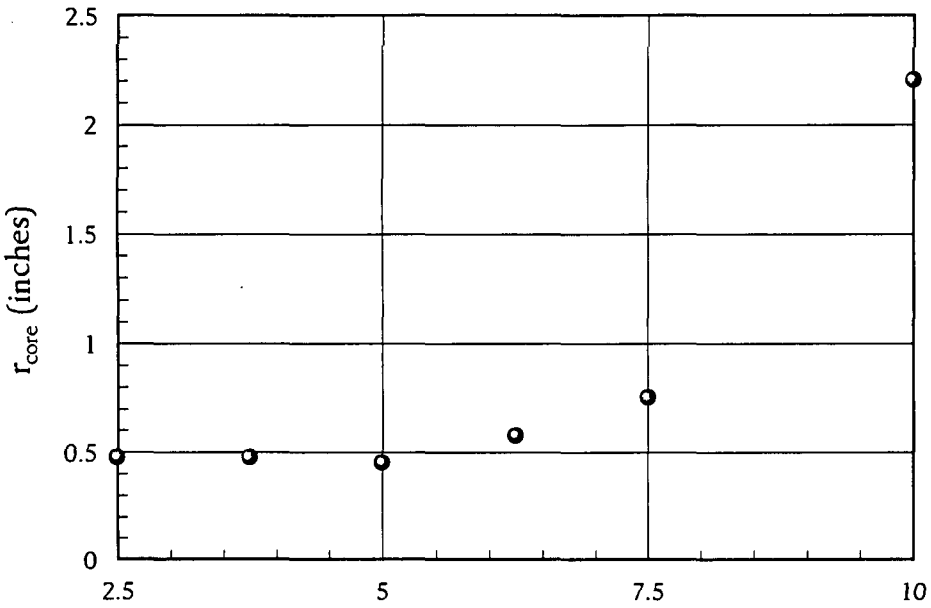


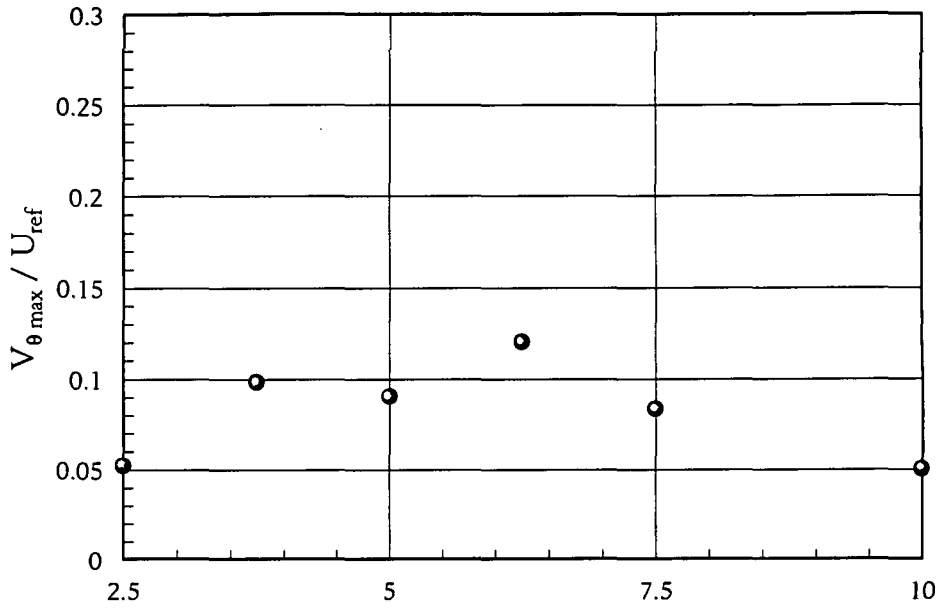


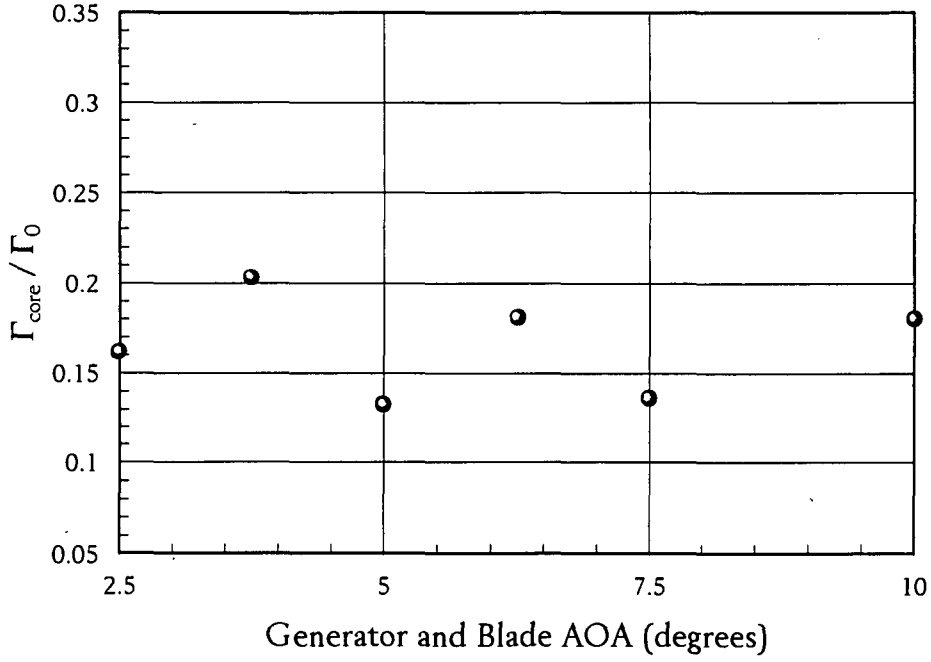


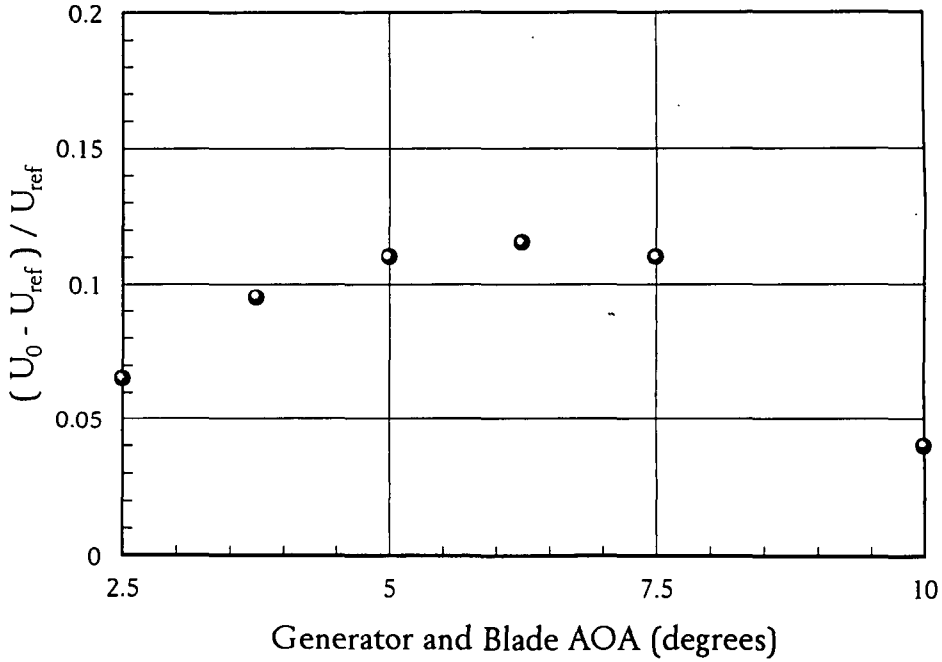


**Figure 5:** Vortex Core Parameters as a Function of AOA at x/c = 30 with $\Delta$ = -1"

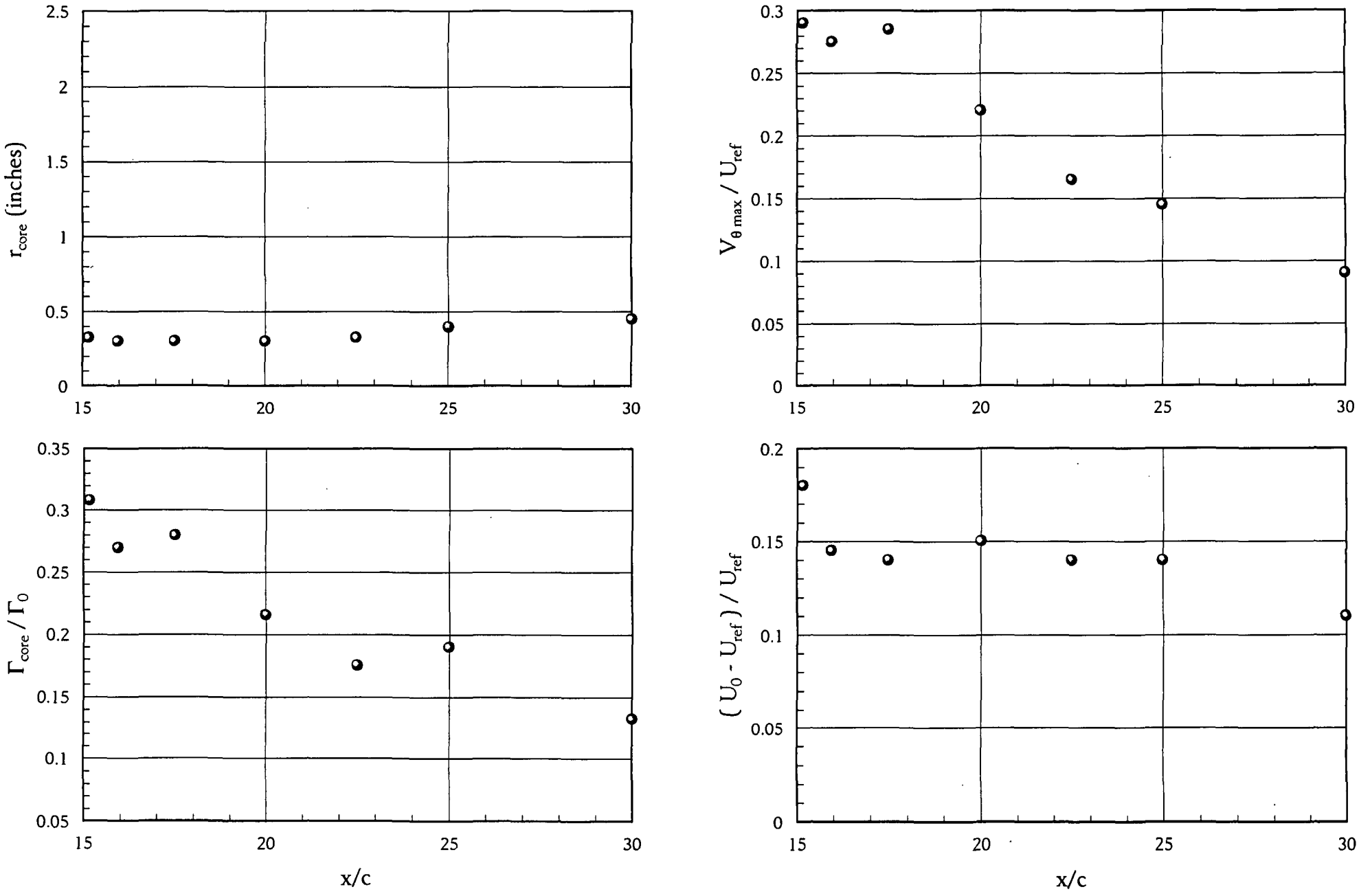


**Figure 6:** Vortex Core Parameters as a Function of x/c for $\Delta$ = -1" with Vortex Generator at 5° and Interaction Blade at 5°

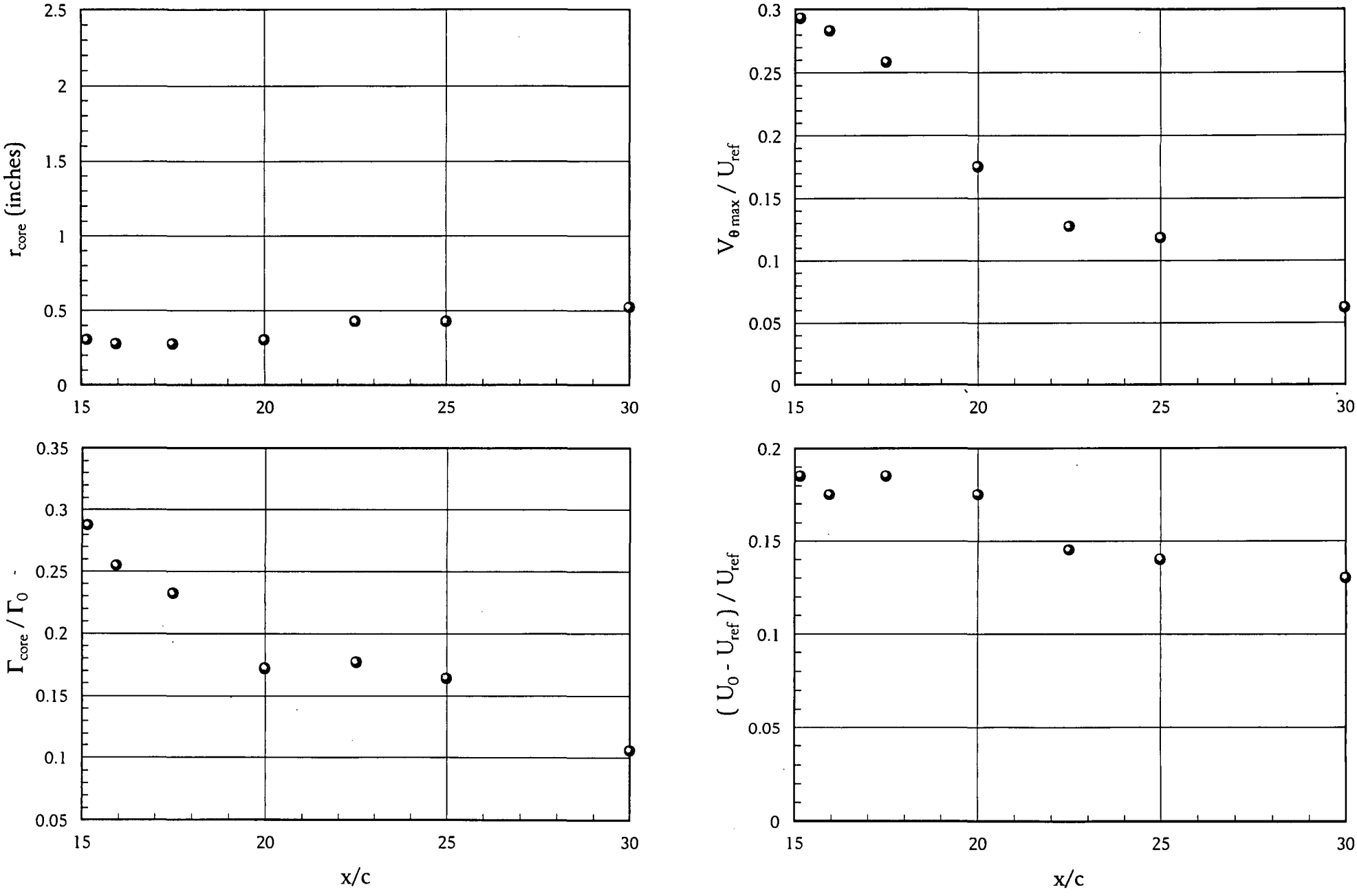


**Figure 7:** Vortex Core Parameters as a Function of x/c for $\Delta$ = 1" with Vortex Generator at 5° and Interaction Blade at 5°

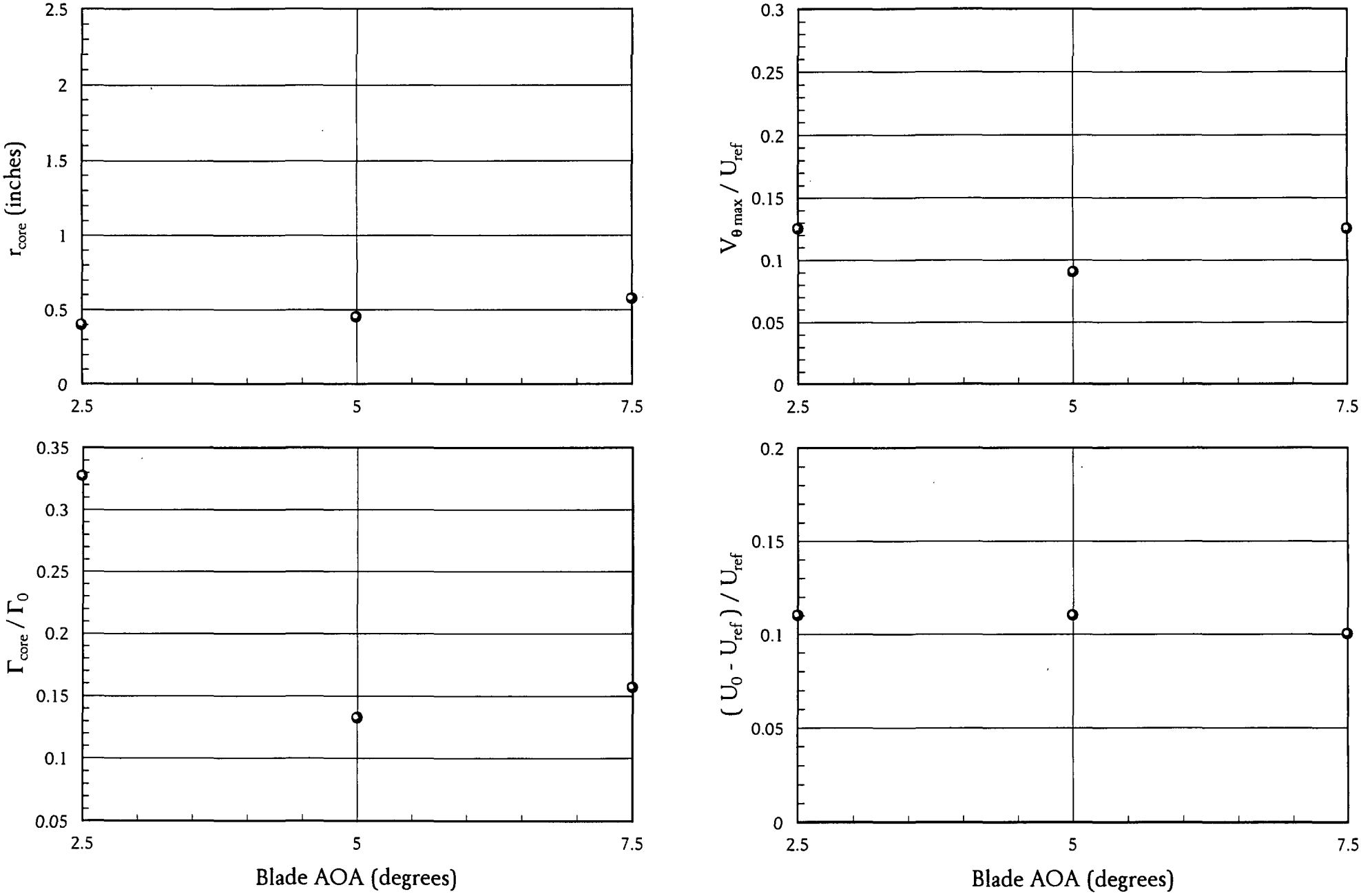


**Figure 8:** Vortex Core Parameters as a Function of Interaction Blade AOA for $\Delta$ = -1" with Vortex Generator at 5°

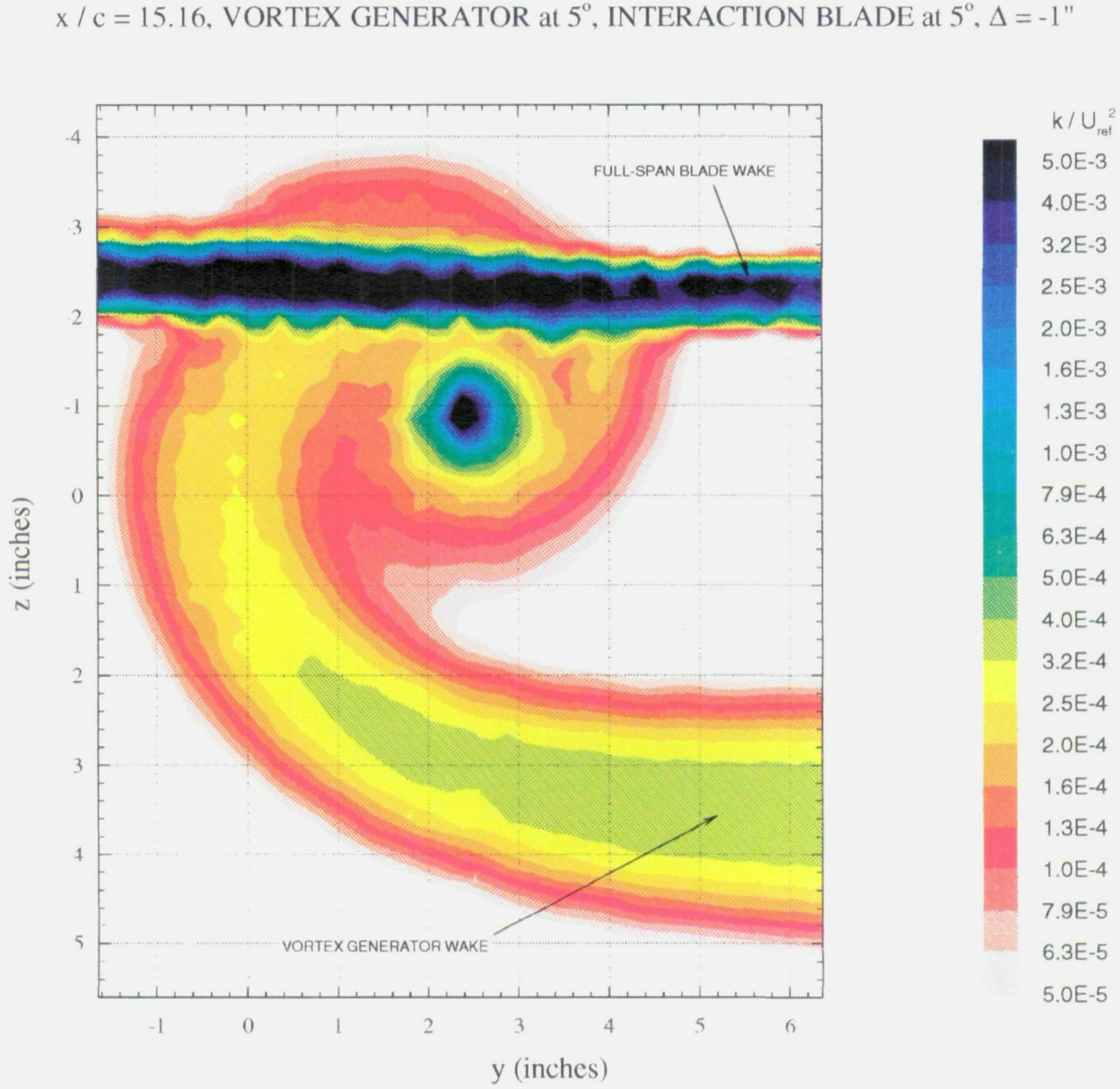


**Figure 9:** Contours of turbulent kinetic energy ($k/U_{ref}^2$)

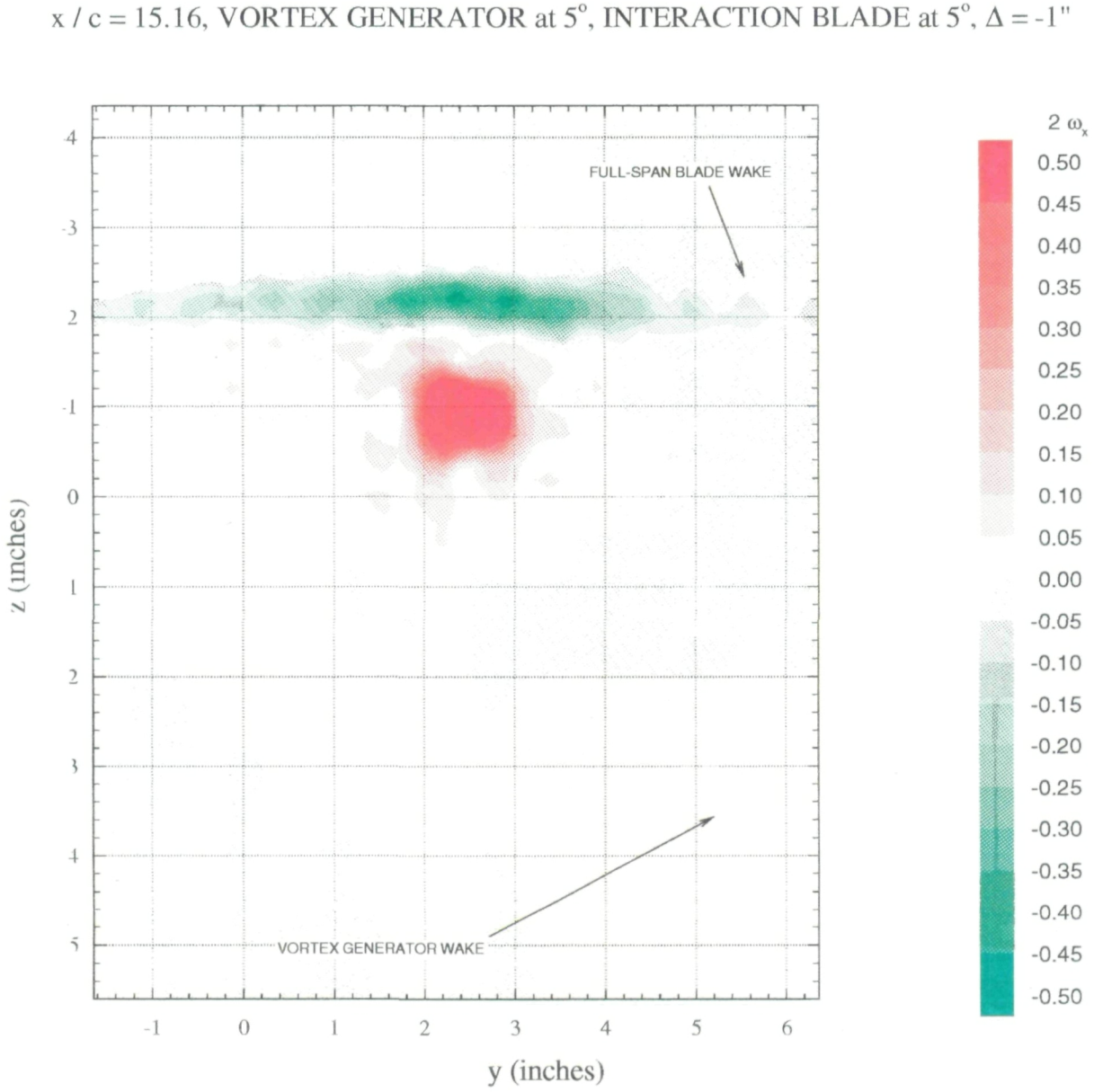


**Figure 10:** Contours of axial vorticity ( $[\partial W/\partial y - \partial V/\partial x]/U_{ref}$ ) with units of 1/inch

**Figure 11:** Contours of turbulent kinetic energy ($k/U_{ref}^2$)

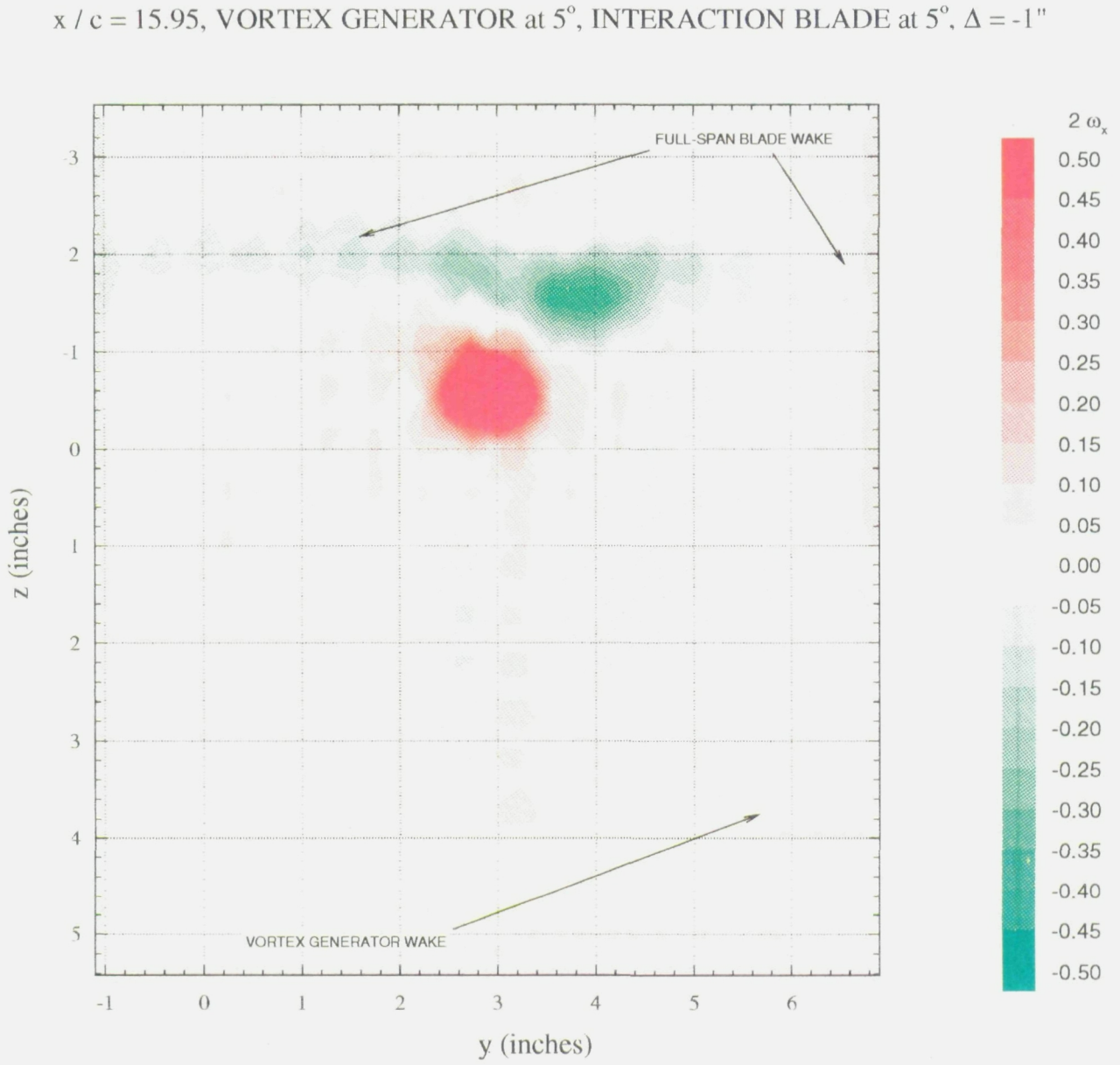


**Figure 12:** Contours of axial vorticity ( $[\partial W/\partial y - \partial V/\partial x]/U_{ref}$ ) with units of 1/inch

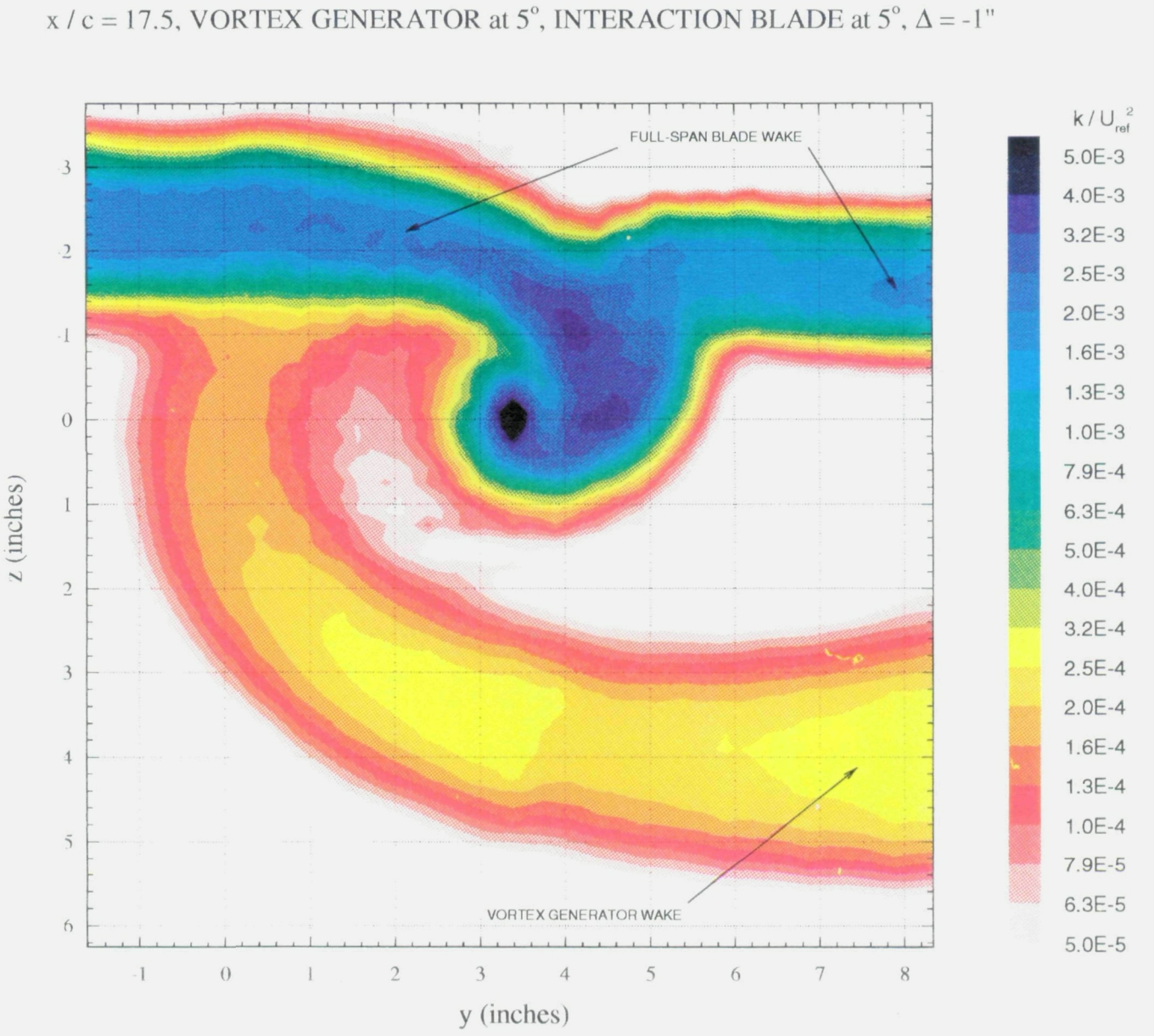


**Figure 13:** Contours of turbulent kinetic energy ($k/U_{ref}^2$)

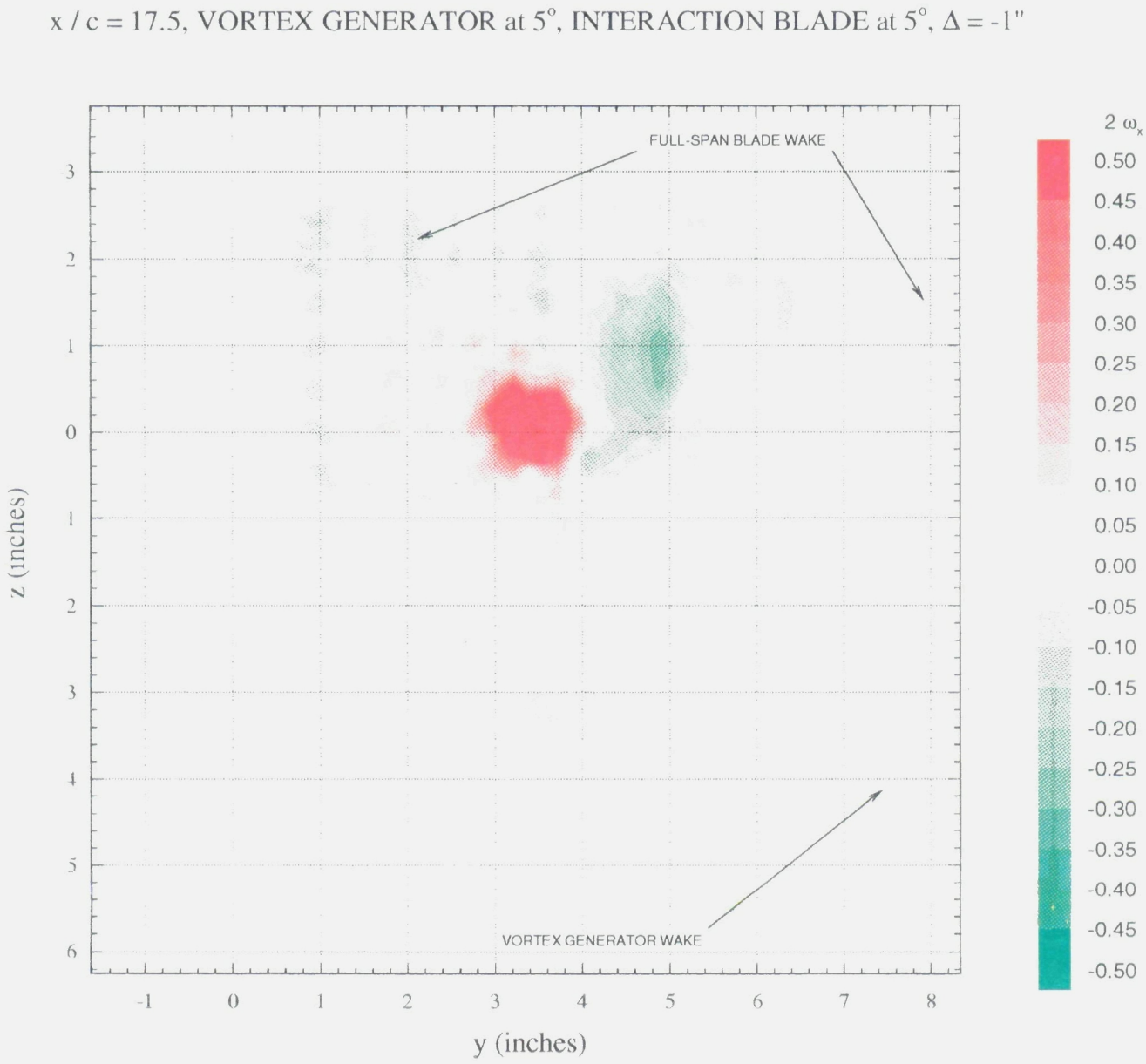


**Figure 14:** Contours of axial vorticity ( $[\partial W/\partial y - \partial V/\partial x]/U_{ref}$ ) with units of 1/inch

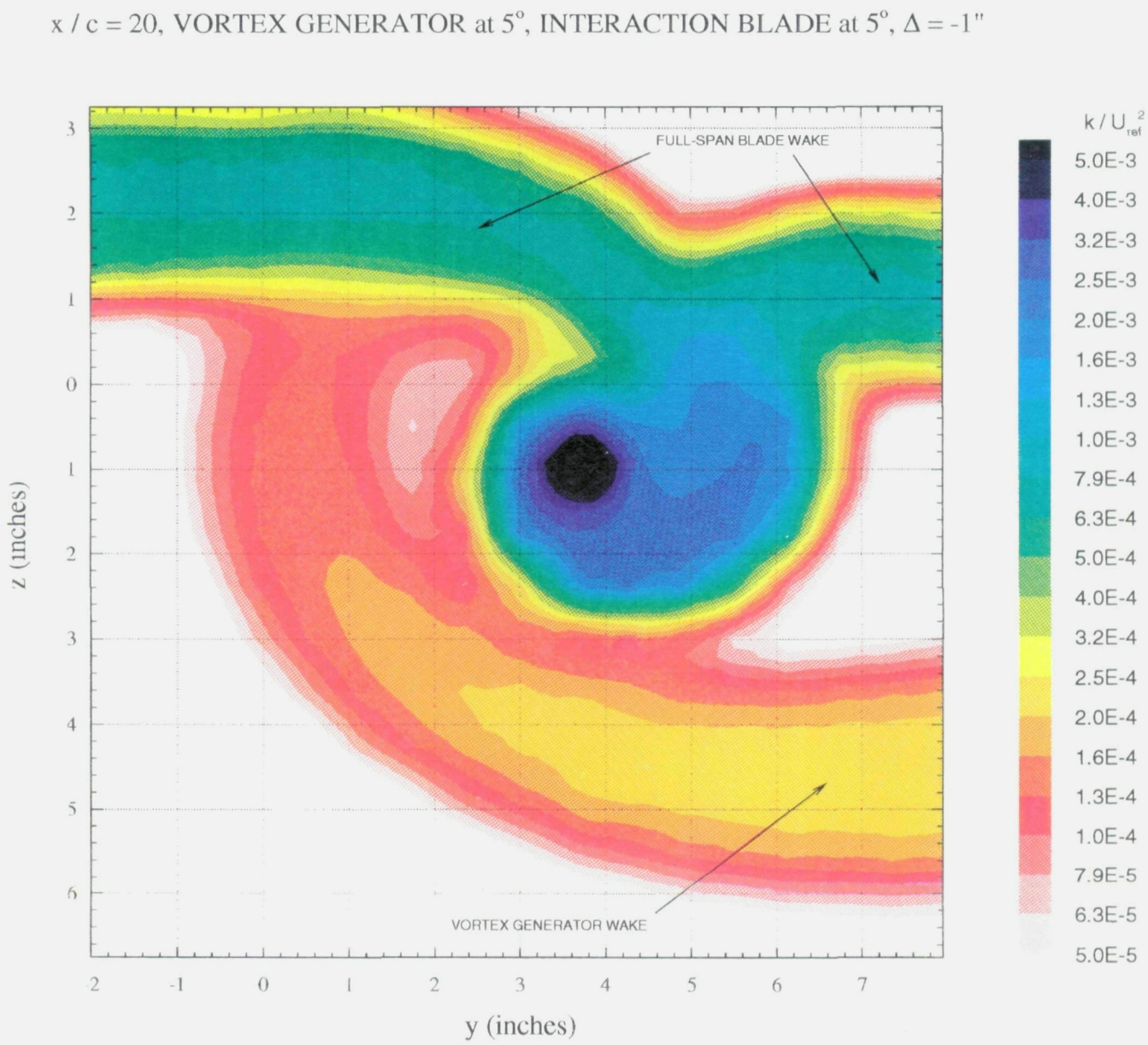


**Figure 15:** Contours of turbulent kinetic energy ($k/U_{ref}^2$)

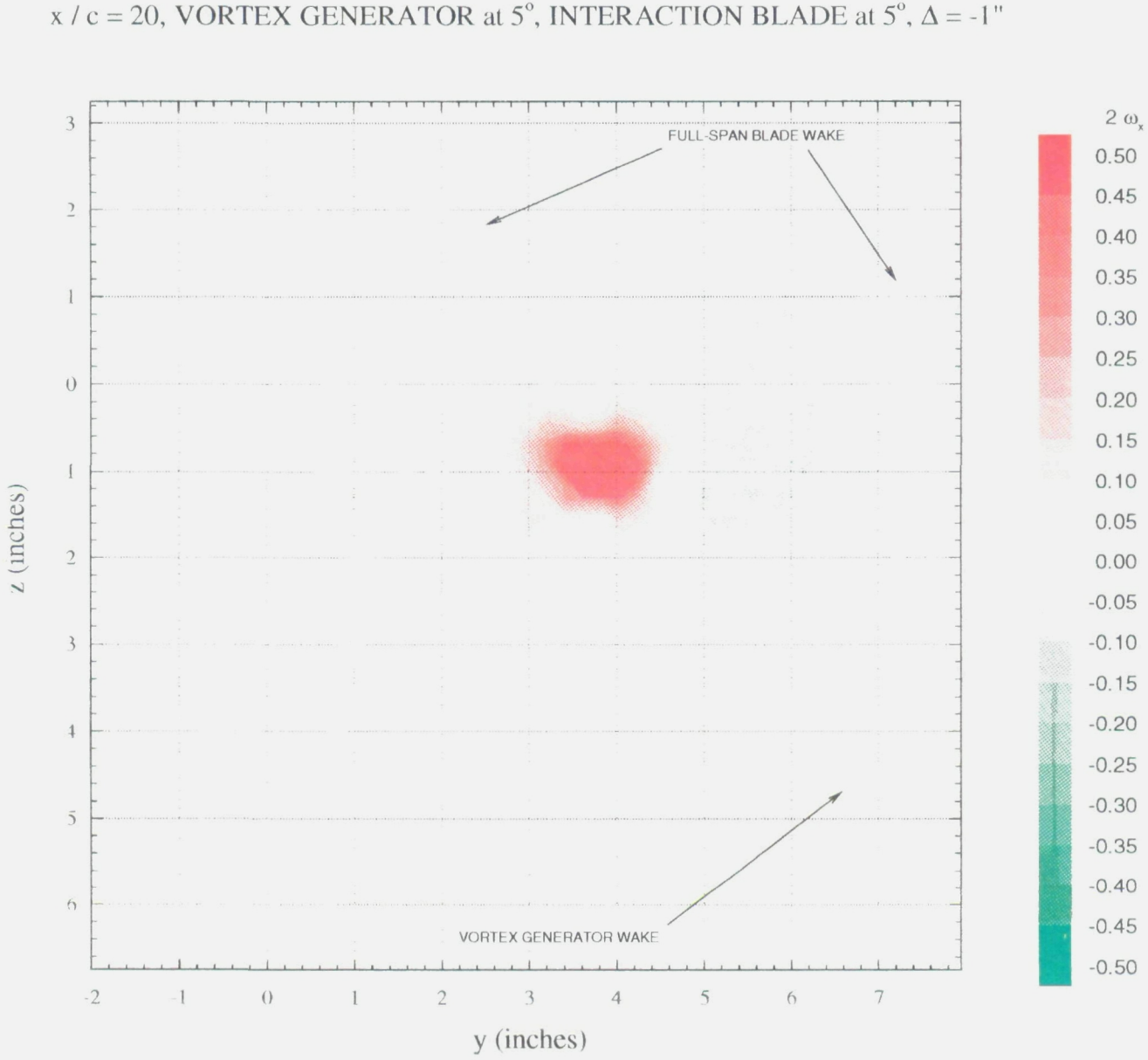


**Figure 16:** Contours of axial vorticity ( $[\partial W/\partial y - \partial V/\partial x]/U_{ref}$ ) with units of 1/inch

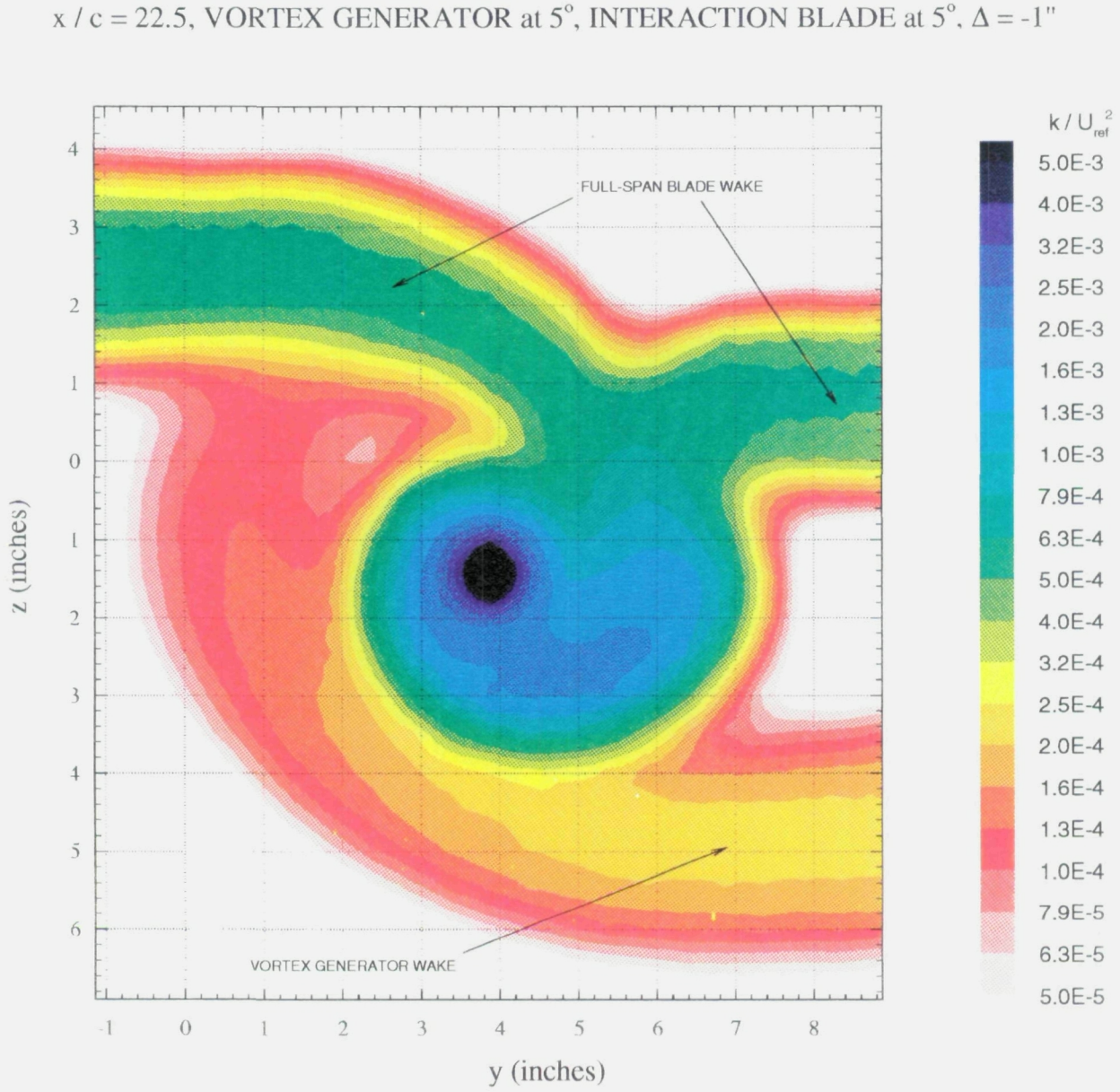


**Figure 17:** Contours of turbulent kinetic energy ($k/U_{ref}^2$)

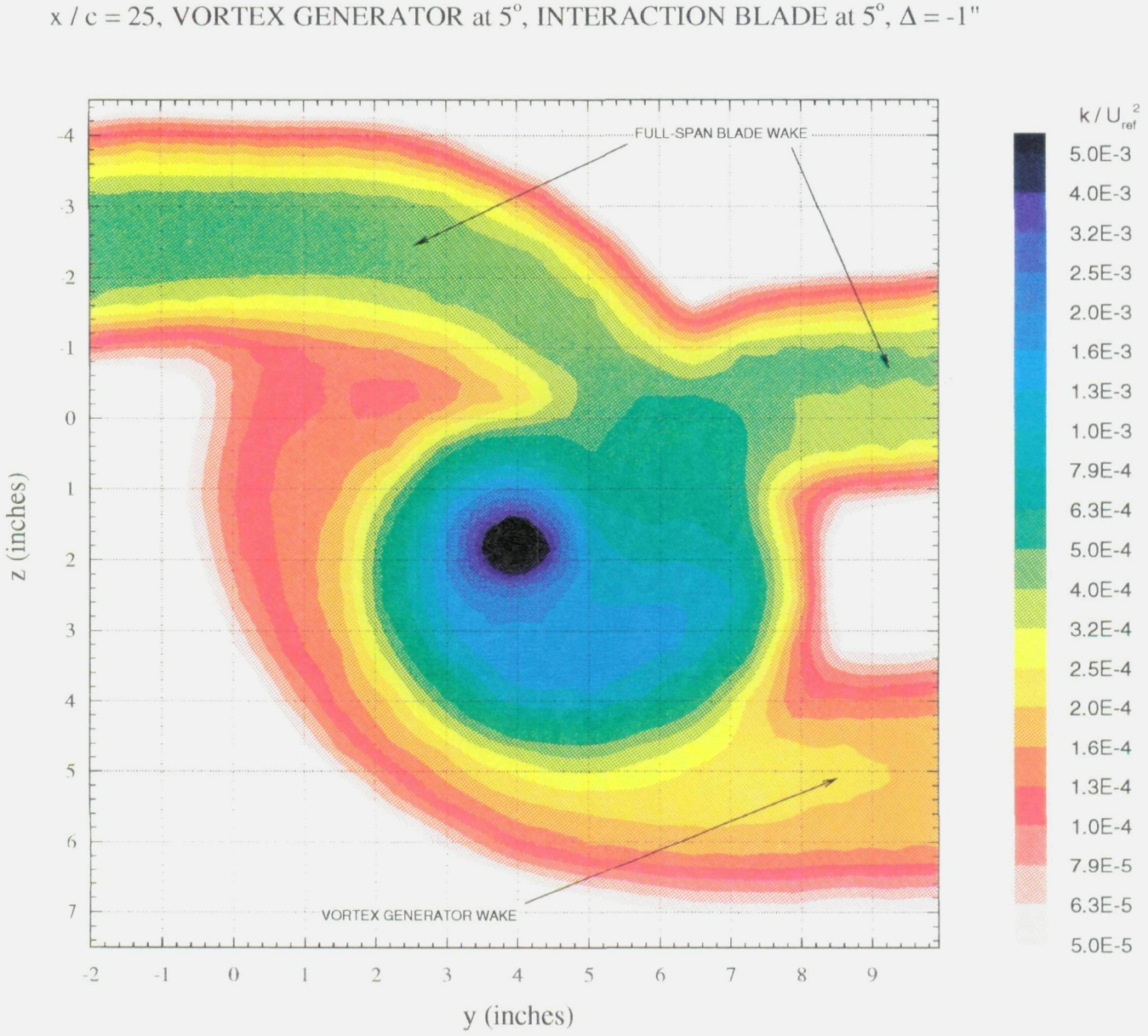


**Figure 18:** Contours of turbulent kinetic energy ($k/U_{ref}^2$)

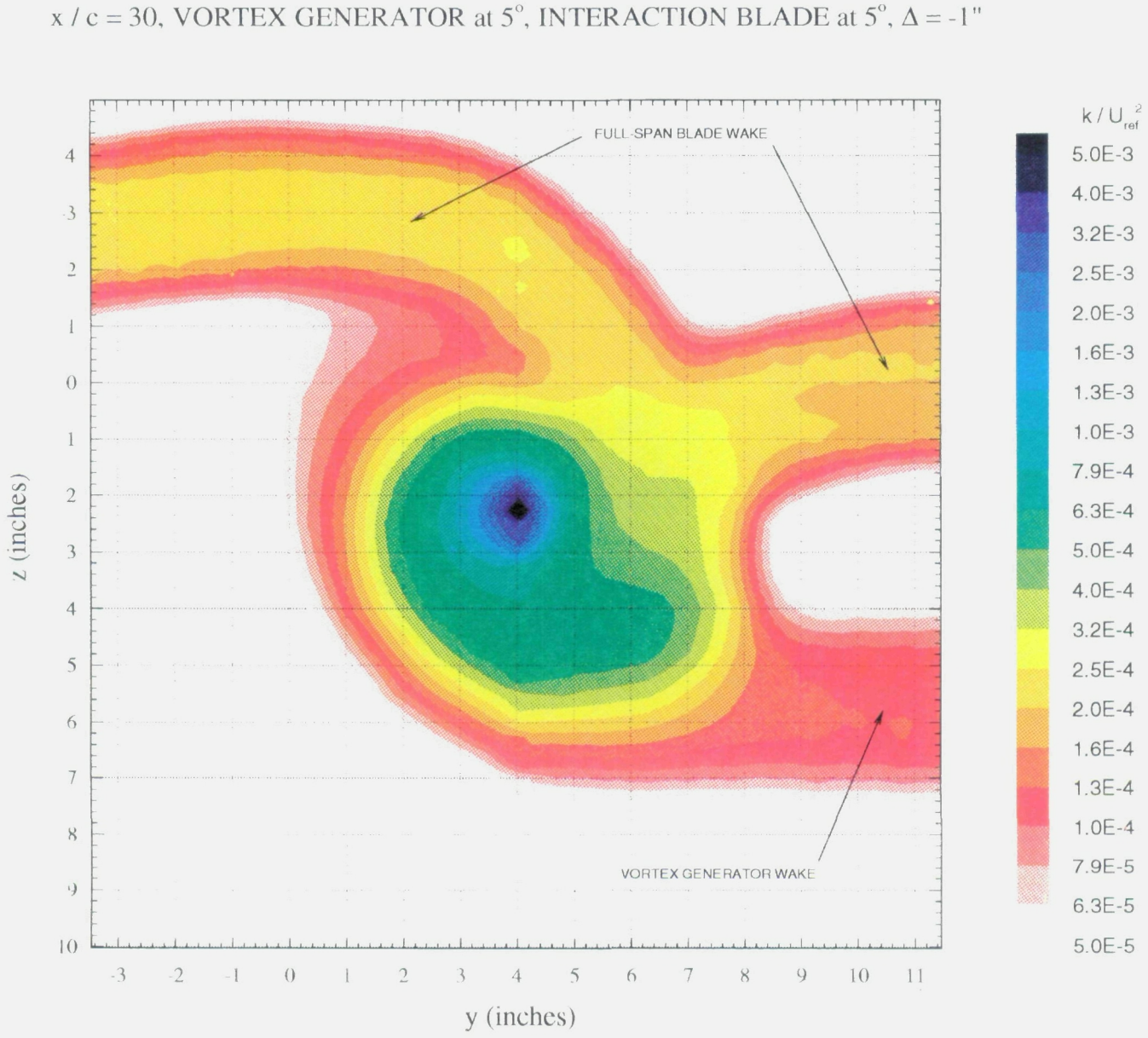


**Figure 19:** Contours of turbulent kinetic energy ($k/U_{ref}^2$)

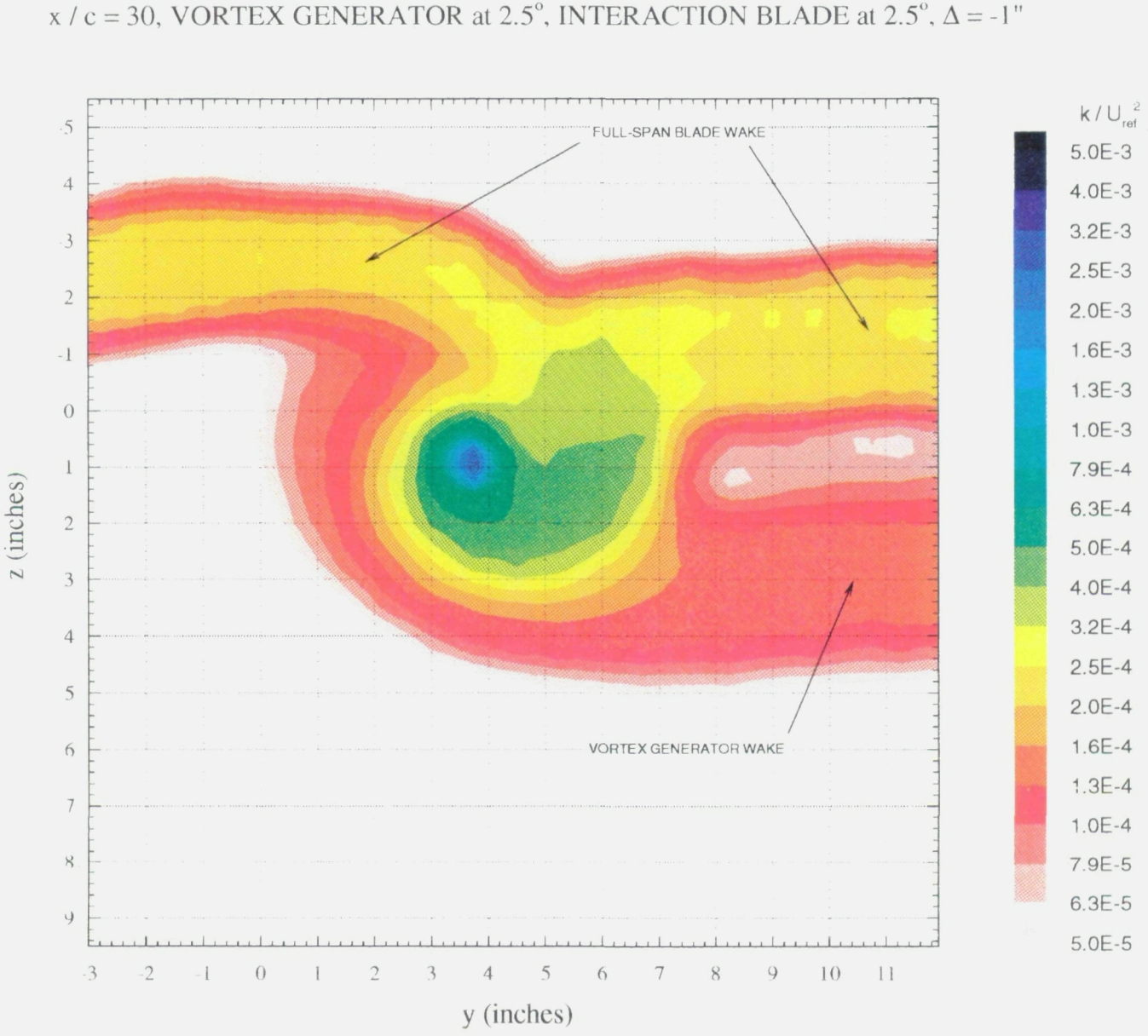


**Figure 20:** Contours of turbulent kinetic energy ($k/U_{ref}^2$)

x / c = 30, VORTEX GENERATOR at 5°, INTERACTION BLADE at 5°, Δ = -1"

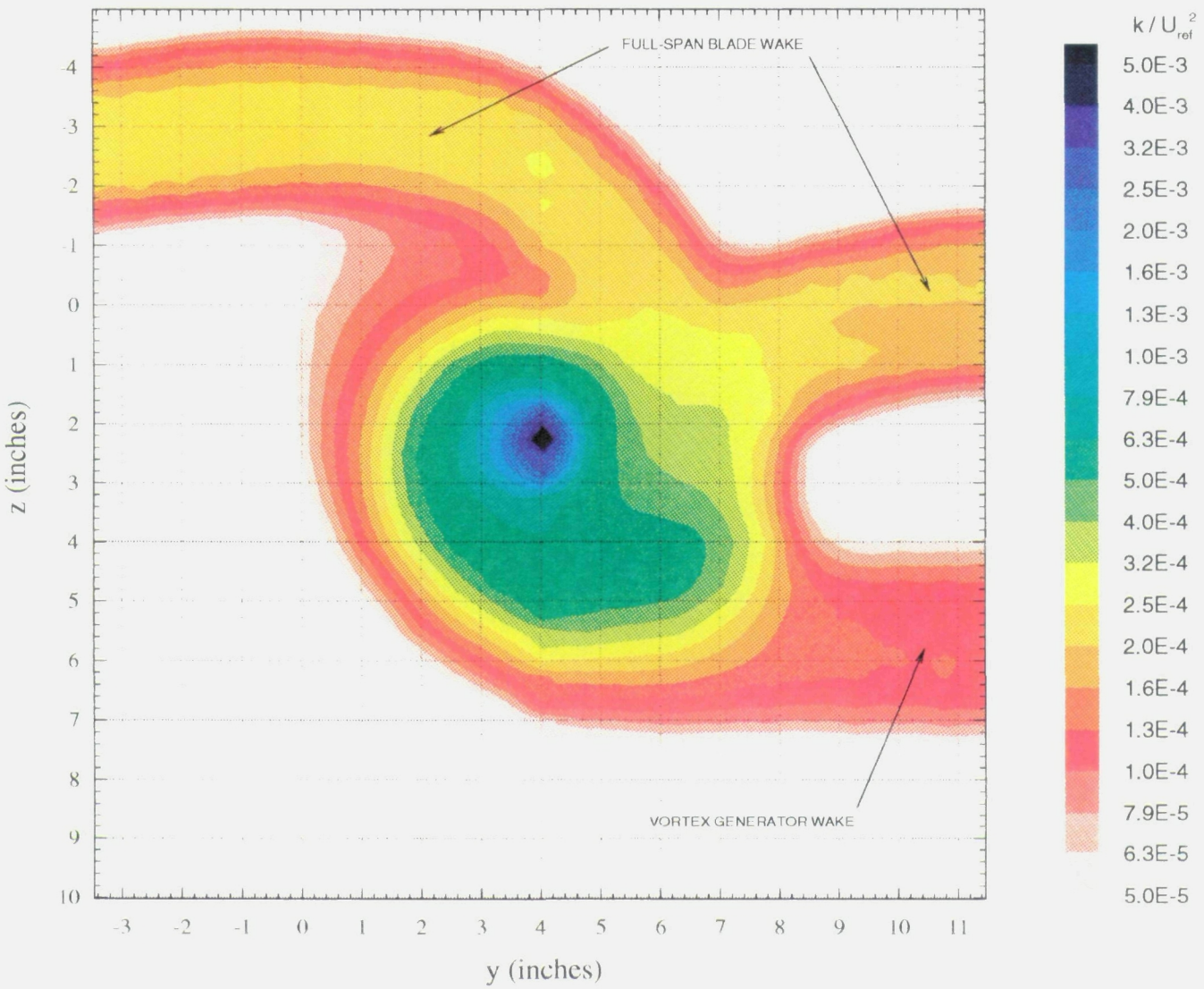


**Figure 21:** Contours of turbulent kinetic energy ($k/U_{ref}^2$)

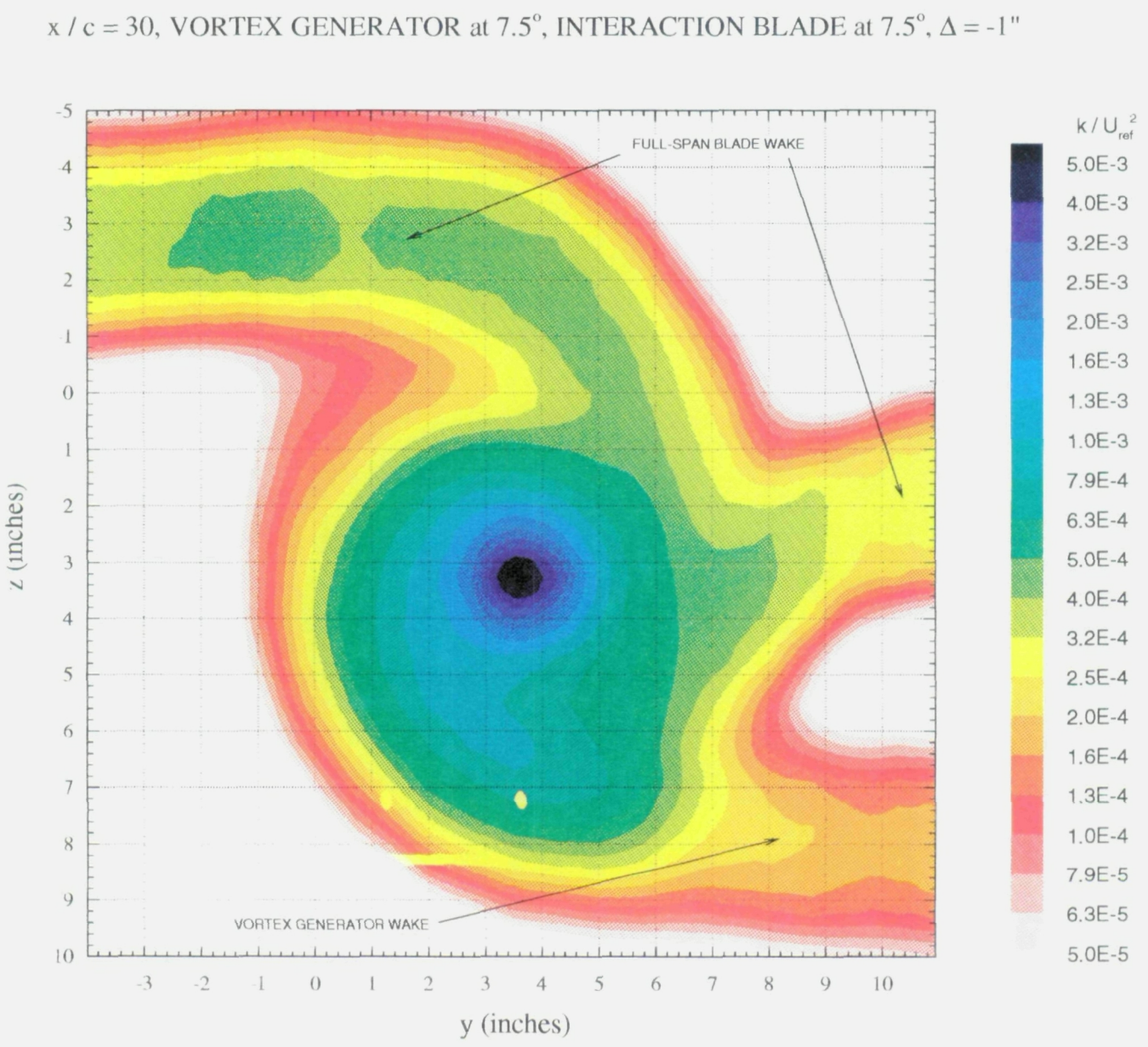


**Figure 22:** Contours of turbulent kinetic energy ($k/U_{ref}^2$)

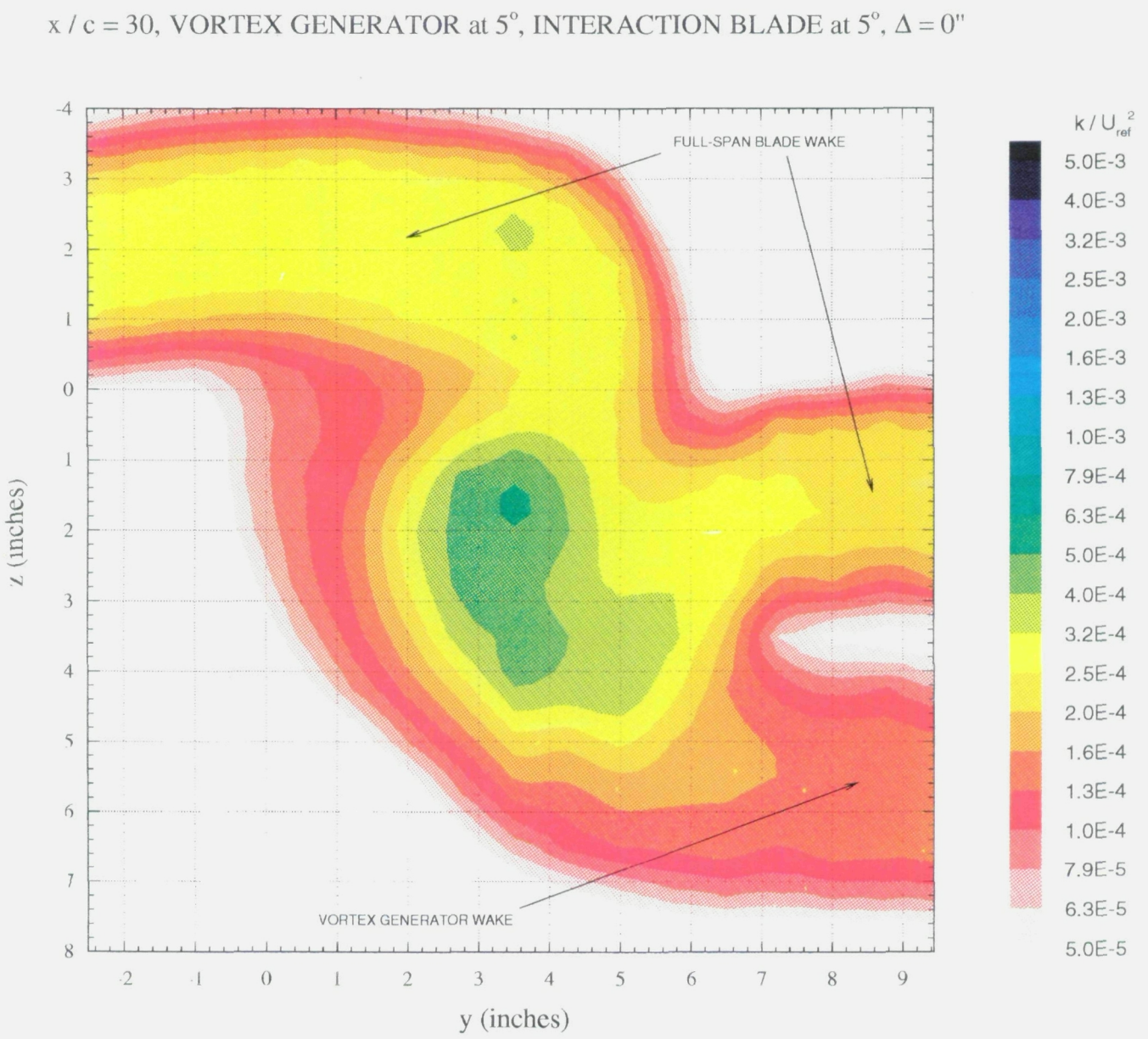


**Figure 23:** Contours of turbulent kinetic energy ($k/U_{ref}^2$)

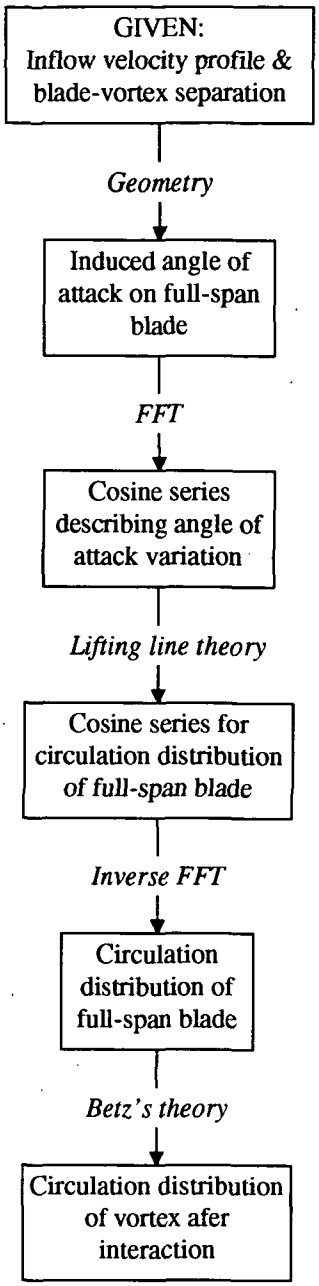


**Figure 24:** Summary of interaction theory

Fig 25 (a)

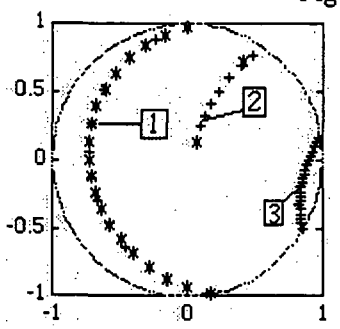


Fig 25 (b)

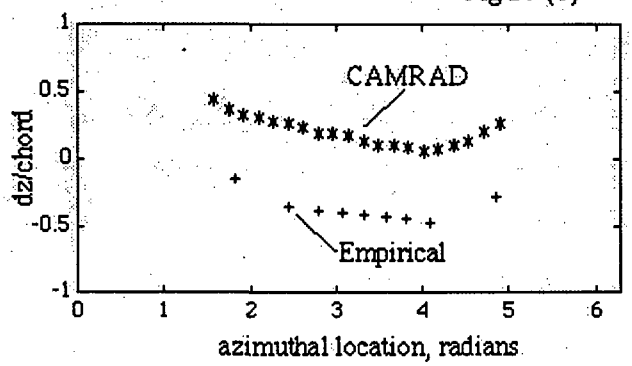


Figure 25: Showing the loci of the *first following* blade vortex intercation in (a) the rotor disc plane and (b) the vertical plane. * CAMRAD data, + empirical method.

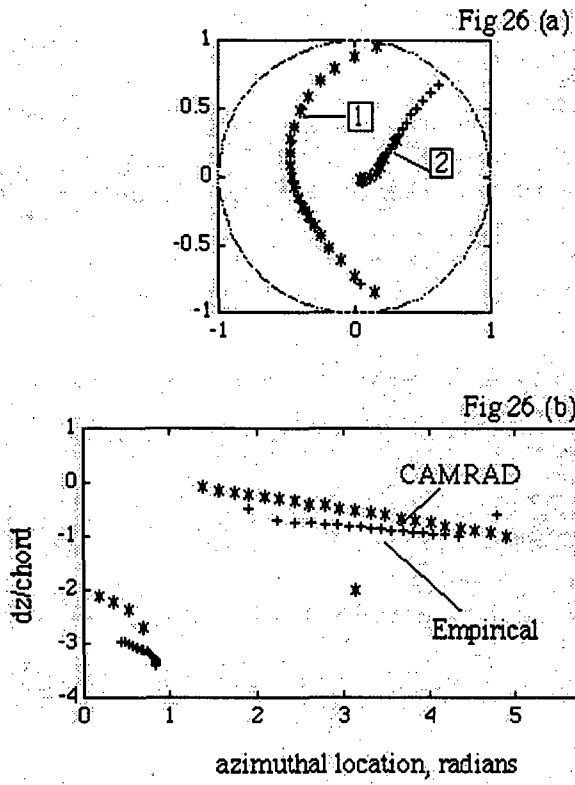


Figure 26: Showing the loci of the *second following* blade vortex interaction in (a) the rotor disc plane and (b) the vertical plane. * CAMRAD data, + empirical method.

Fig 27 (a)

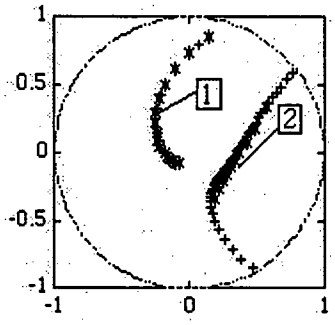


Fig 27 (b)

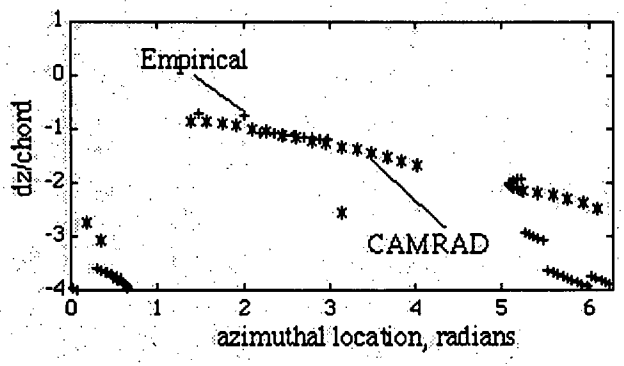


Figure 27: Showing the loci of the *third following* blade vortex intercation in (a) the rotor disc plane and (b) the vertical plane. * CAMRAD data, + empirical method.

# Controlling Trailing Tip Vortices

Christopher M. Weisser
Virginia Polytechnic Institute and
State University, Blacksburg, VA

**1995 Mid-Atlantic Student Conference**
April 21-22, 1995 / George Washington
University, NASA Langley Campus

# Controlling Trailing Tip Vortices

CHRISTOPHER M. WEISSER

*Department of Aerospace and Ocean Engineering*

*Virginia Polytechnic Institute and State*

*University, Blacksburg, Va.*

## Abstract

This study was undertaken to formulate an empirical prescription for obtaining a given core size based on a set of wing-tips. These wing-tips were designed such that they vary in one-dimension. This was done such that a change in the core size could be related to only one parameter. The main interest of this investigation was to find a set of wing-tips that would increase the vortex core size to a desired level. It was also important that the increasing the core size have no effect on the lift of the entire wing section. After numerous trials of different design wing-tips, a circular tip-plate was found to yield the desired results.

## Nomenclature

| | |
|---|---|
| $\alpha$ | angle of attack |
| $\Gamma$ | circulation around wing |
| $\rho_{ref}$ | free-stream density |
| AR | aspect ratio of the unmodified wing, $b^2/S$ |
| b | wingspan of the unmodified wing |

| | |
|---|---|
| c | chord length |
| q | dynamic pressure |
| r | vertical distance from core center |
| S | wing area of the unmodified wing |
| $U_{ref}$ | free-stream velocity |
| w | tangential velocity component |
| $w/U_{ref}$ | ratio of the tangential velocity to the free-stream velocity |

## Introduction

Aircraft trailing vortices have become of great interest to the aviation industry in recent years. The aircraft industry is taking precautions in avoidance of wake-aircraft interactions while the helicopter industry is interested reducing the noise associated with the vortices. Due to this insight, a considerable amount of research is being performed to better understand the trailing tip vortex to control the vortex core size. Studies such as those performed by Marchman and Uzel at Virginia Polytechnic Institute and State University and Heyson, Riebe, and Fulton at the NASA Langley Research Center include the use of variable wing-tips to change the size of the vortex. These wing-tip modifications have concluded varying degrees of success. The modifications used include wing-tips such as endplates, decelerating chutes, and extensions.

## Experimental Procedure

An experimental investigation of the effects of seventeen wing-tips on a NACA 0012 wing section's trailing vortex was performed in the Virginia Tech Blow-Down Tunnel. The tunnel has a three foot by two foot test section and the test section spans twenty-two feet. Figure 1 shows an internal view of the test section. Measurements were taken at a distance of ten chord lengths downstream of the wing's trailing edge.

Measurement data was reduced from a calibrated quad-wire hot wire anemometer. The hot-wire probe was used to measure the three components of velocity of the trailing vortex. The probe was mounted to a probe stem, shown in Figure 2, which was in turn mounted to the traversing system shown in Figure 3. The traverse system allowed both horizontal and vertical movements of the probe across the test section area. This allowed for the determination of the vortex core center which is where the profile was taken.

The wing used in this experimental investigation was an 8-inch chord, aluminum, NACA 0012 wing section four feet in length. This wing is similar to the wing that was used in Reference 3. The wing section was held in place by the apparatus shown in Figure 4. This apparatus allowed the wing to be set at any desired aspect ratio and angle of attack, for this investigation an aspect ratio of 2.5 and an angle of attack of 5° was chosen. The 5° angle of attack provided a strong vortex that was simpler to measure and the aspect ratio of 2.5 guaranteed

that there would be no vortex wall interaction at ten chord lengths downstream. All tests were run at the same angle of attack and at a dynamic pressure of 1.44 inches of water.

Sixteen wing modifications were used as well as the plain wing case. These wing modifications were grouped into five categories: 1) elliptical tips, 2) full-endplates, 3) flat-plate subwings, 4) half-endplates, and 5) circular tip-plates. Thirty-six wing-tips were originally made with one varying parameter of each set. All the wing-tips were mounted to the end of the wing, except for the circular tip-plates which were mounted perpendicular to the flow at the tip of the trailing edge. The number of wing-tips tested of each set was determined based on the effectiveness of the design of the wing-tip.

The first set of wing-tips were of the elliptical tip design and are shown in Figure 5. These tips were made of wood and were sanded into a rectangular ellipse shape. These tips' profiles satisfy the ellipse equation and were made to fit a template. This set of wing-tips have an accuracy of $\pm 0.02$ inches according to the templates made and vary in span from one-quarter to two inches with a chord of eight inches.

The endplate design wing-tips are shown in Figure 6. They were constructed of one-eighth inch, aluminum sheet metal. These wing-tips had a chord length of eight inches and introduced no twist or camber. The wing-tips had a semicircular leading edge and a blunt trailing edge. The wing-tips of this category ranged in height from one-quarter to four inches.

The subwings, shown in Figure 7, were constructed of 1/16 inch, steel sheet metal and varied in span from one-half to five inches, each having a chord of two inches. The subwings were mounted such that the half chord of the subwing matched with the quarter chord of the wing.

The next two wing-tips were constructed during testing in the search for a wing-tip that produced satisfactory results. The first of which was a half-endplate design shown in Figure 8. This wing-tip was constructed the same as the full endplate above except the bottom of the plate was cut to the shape of a NACA 0012 half section. Only two of these were constructed before moving on to the next style of wing-tip. The sizes of these two tips were three-quarters of an inch and one and three quarters of an inch in height from the chord line.

The final wing-tip tested was the circular tip-plate shown in Figure 9. This circular plate was constructed of 1/16 inch sheet metal and was attached to an adapter mounted on the tip of the wing section. The adapter allowed the tip-plate to be mounted perpendicular to the trailing edge of the wing. The center of the circular plate was just inboard of the wing-tip and the tips ranged in diameter from one to three inches.

## Results and Discussion

The data from this investigation can be seen in Figures 10 - 16 as the ratio of the tangential velocity profiles, $w/U_{ref}$, versus the vertical distance, y in inches, at ten chord lengths downstream of the wing. Figure 10 shows the tangential velocity profile for the Elliptical wing-

tips plotted against the plain wing case. From this plot, one notes that the peak tangential velocity increases slightly with increasing wing-tip size. The peak to peak distance that represents the vortex core size is slightly decreasing. This change is fairly small and, unfortunately, is not the direction of interest.

Figure 11 shows a similar plot for the Endplate wing-tips. In this plot, the tangential velocity decreases, which is the desired case. However, the core size remains almost constant, decreasing only slightly with the increasing height of the endplates. Therefore, this design does not satisfy the requirements of this research either.

The Subwing wing-tip produced interesting results that can be seen in Figure 12. The subwing designs show a little improvement over the previous two cases. The tangential velocity component does indeed decrease as compared to the plane wing for all the cases. However, as the size increased from approximately a 1" subwing, a second vortex core was measured. This is denoted from the dip in tangential velocity before the first peak, and immediately following the second vortex peak. This is most profound in the 3" Subwing case. With a small subwing, the two vortex cores had time to merge by 10c downstream, the distance at which the measurements were taken. However, the larger the subwing, the larger the second core became until there was not enough distance between the wing and 10c for the two cores to merge. Because of this, it was difficult to deduce whether the subwing was producing the desired results.

During testing, the idea of a half-endplate was introduced. This idea was thought to allow the flow to circulate freely from the under-side of the wing while not permitting it to form the vortex on the top side due to the interference of the plate. The results of these wing-tips can be seen in Figure 13. Unfortunately, these tips showed the same results as the full endplates. The half-endplates decreased the tangential velocity flow but did not increase the vortex core size.

One last attempt to increase the vortex core size was made by designing a circular tip-plate attached at the tip of the wing, perpendicular to the flow. The idea behind this wing-tip was to burst the vortex core as it began to develop. The results were astounding and can be seen in Figure 14. Not only did the core size increase but, the tangential velocity decreased at an unbelievable rate. In fact, the tangential velocity ratio becomes astonishingly small with the 3" circular tip-plate. At the same time, the vortex core size grew to over six inches.

In summary of all the tip modifications used, Figure 15 shows the trends in vortex core size with the increasing component of the wing-tip. As shown, there is no real change in the size of the vortex core for the subwings, elliptical tips, endplates, or half-endplates. It is rather fair to say that the small changes are well within the experimental error of this investigation. The one trend that stands out above all the others is the circular tip-plate. Its core size increases almost linearly with increasing diameter.

It is very important that when changing the vortex core size, that the lift developed by the wing not be disturbed. In an attempt to determine the lift on the wing, the circulation was calculated for all the circular tip-plates used above. Where the circulation is calculated as shown in Equation 1 and is directly related to the lift by Equation 2 below:

$$\Gamma = 2\pi r w \qquad (1)$$

$$l = \rho_\infty U_\infty \Gamma \qquad (2)$$

The results of this calculation can be seen in Figure 16. As shown, there is no major change in the circulation around the wing as compared to the plain wing case. This is apparent due to the similarity of the peak circulation at the left and right endpoints. This demonstrates that this wing-tip is fully effective in enlarging the vortex core size while not harming any lift on the wing. The only question remaining about this design of wing-tip is whether the drag induced by the circular tip-plate is less than or greater than the trailing vortex drag of the plane wing.

## Conclusions

This study has concluded that wing-tips do have an impact on the size and strength of a vortex core. It has also been concluded that different design wing-tips have distinct effects on the vortex core. Of all the design tips tested in this research project, the circular tip-plate wing-tip design has proven to be the most valuable. The circular tip-plate design does in fact increase the vortex core size without harming the lift on the wing. More research is needed on this subject for the exact empirical relation between the vortex core size and the plate diameter.

Further Study is also needed to deduce the lift and drag information associated with this wing-tip design.

## Acknowledgments

I would like to thank Dr. William Devenport, Ken Whittmer, and Mark Engel of Virginia Polytechnic Institute and State University for the equipment used in this investigation and also for their patience in guidance through this project. Financial support for some of the instrumentation and supplies used in this study was provided by NASA Langley through grant NAG-1-1539.

## References

1. Bertin, J.J. and Smith, M.L., Aerodynamics for Engineers, Second Edition, Prentice Hall, New Jersey, 1989, pp. 96-7.
2. Heyson, H.H., Riebe, G.D., and Fulton, C.L., "Theoretical Parametric Study of the Relative Advantages of Winglets and Wing-Tip Extensions," NASA TP-1020, 1977.
3. Marchman, J.F., III and Uzel, J.N., "Effects of Several Wing Tip Modifications on a Trailing Vortex," *Journal of Aircraft*, Vol. 9, No. 9, September 1972, pp. 684-686.

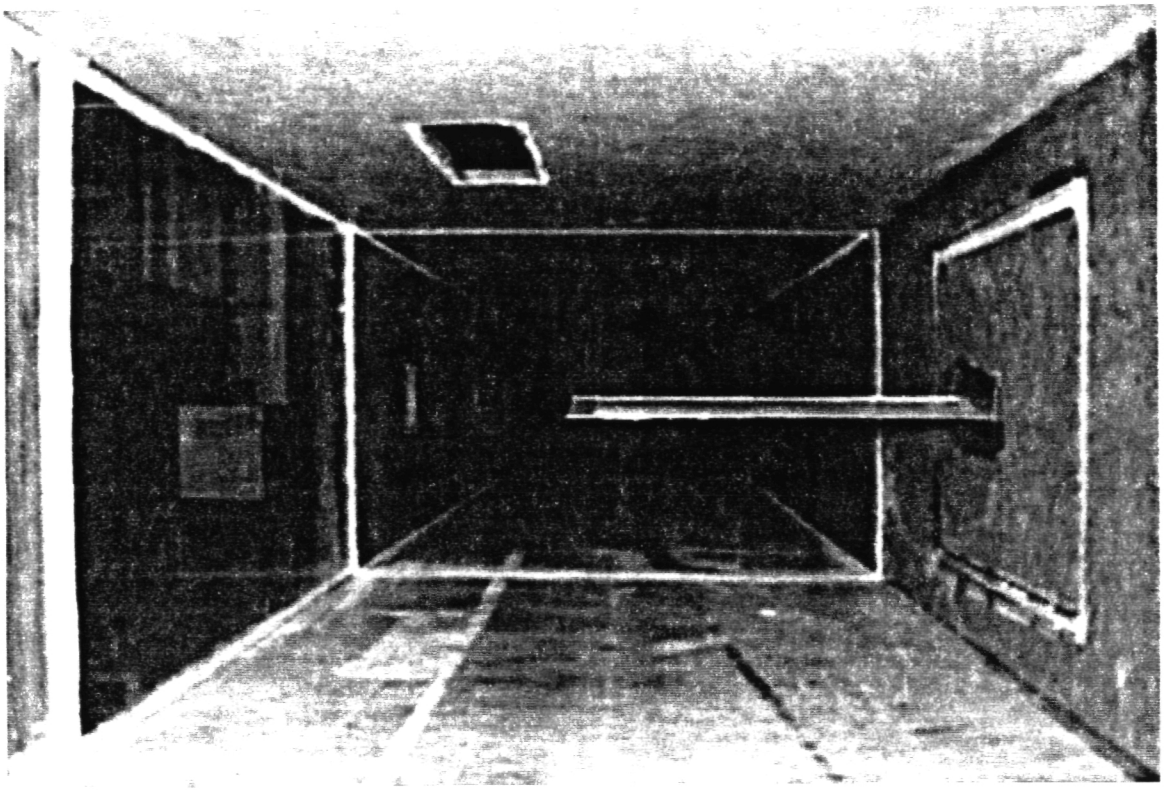

Figure 1: Virginia Tech Blow Down Tunnel test section

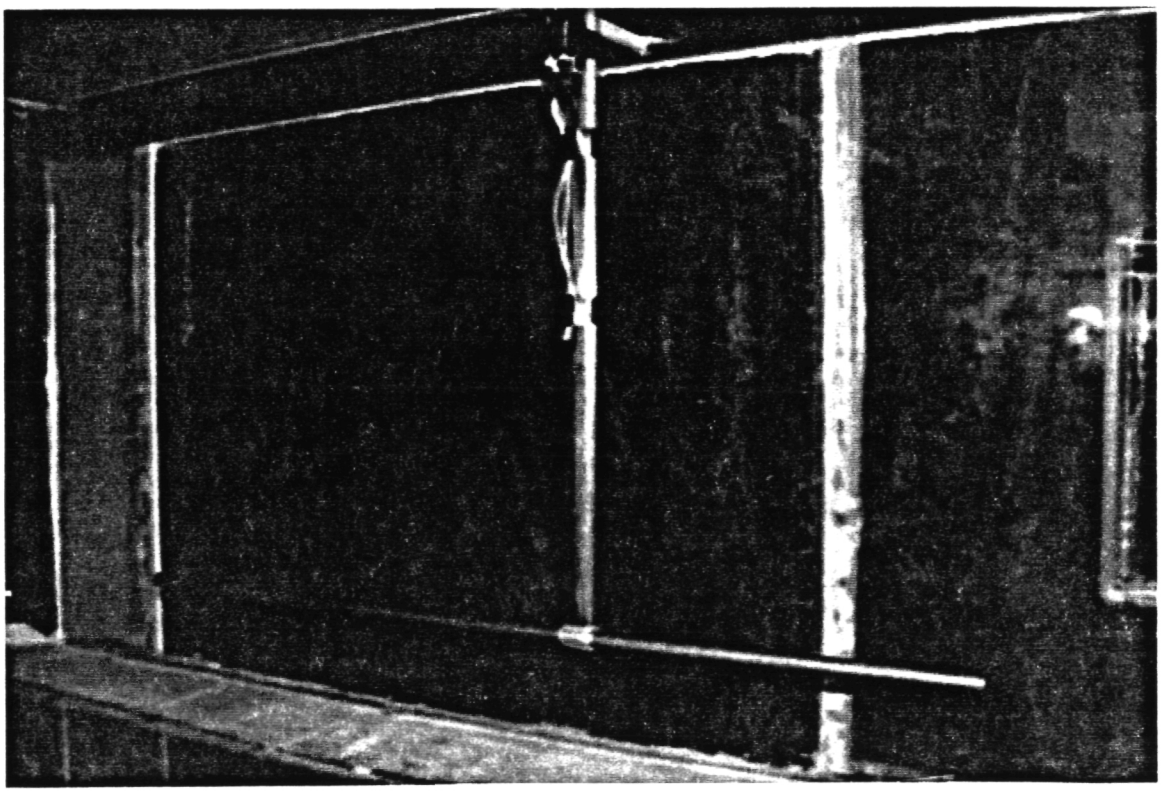

Figure 2: Hot-wire anemometer probe stem

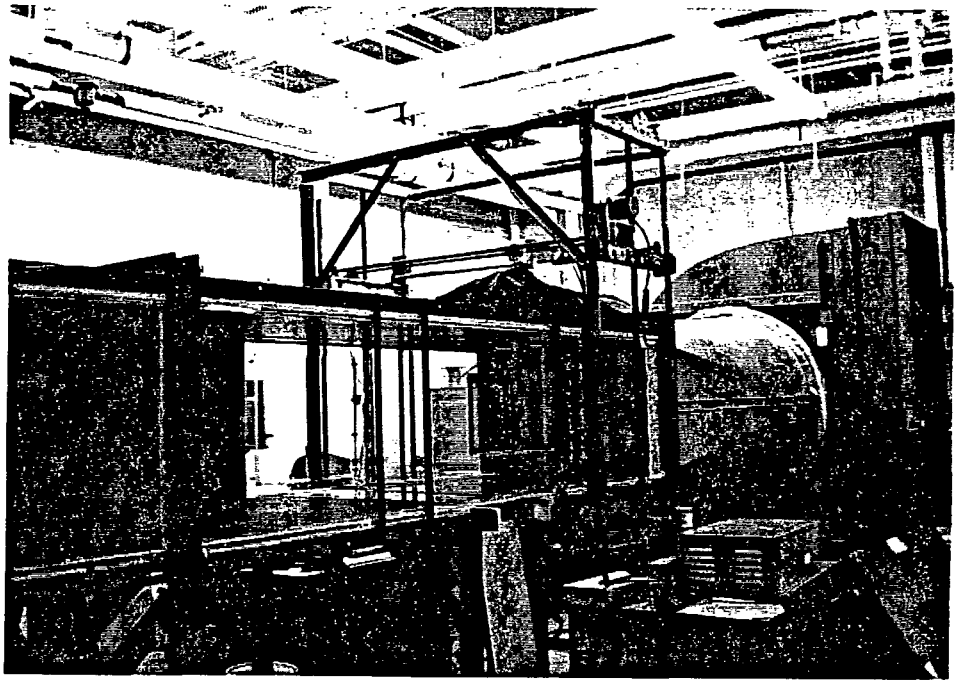

Figure 3: Traversing system

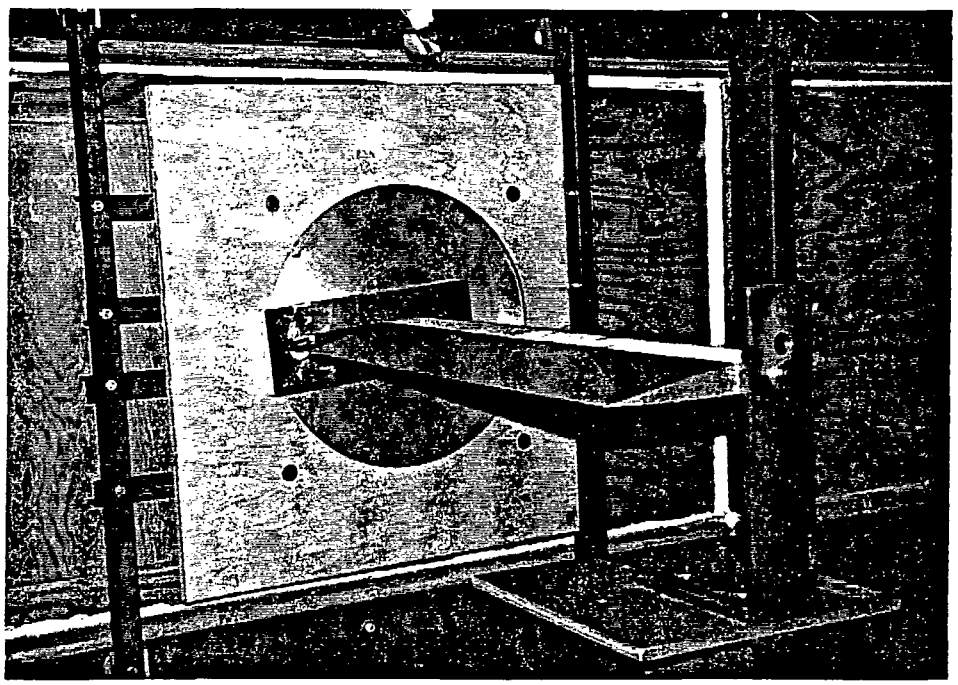

Figure 4: Wing mounting apparatus

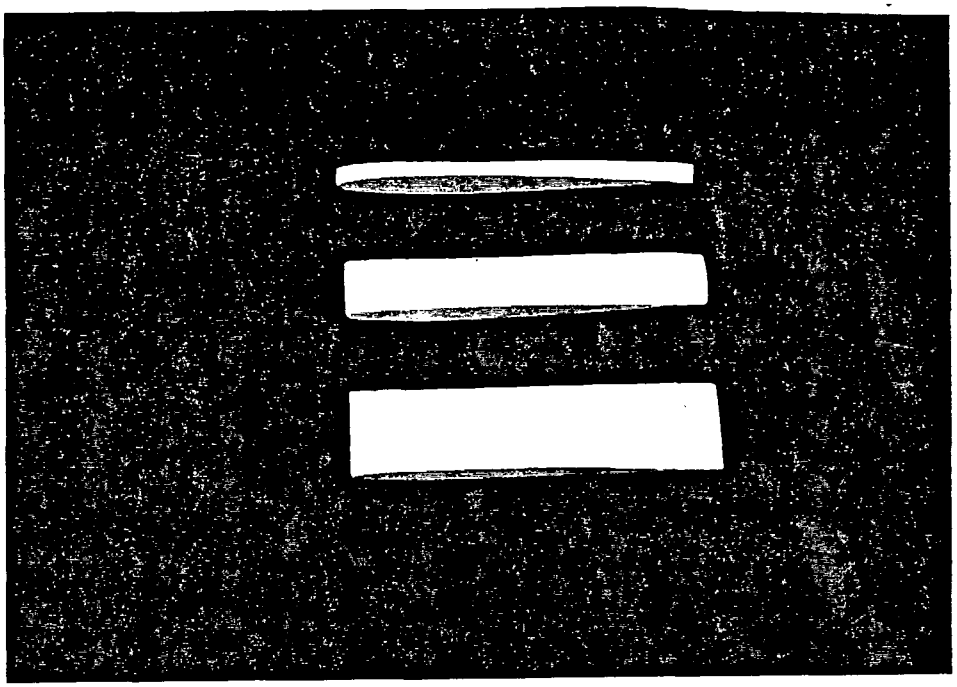

Figure 5: Elliptical wing-tips (top to bottom: 0.5", 1.25", 2")

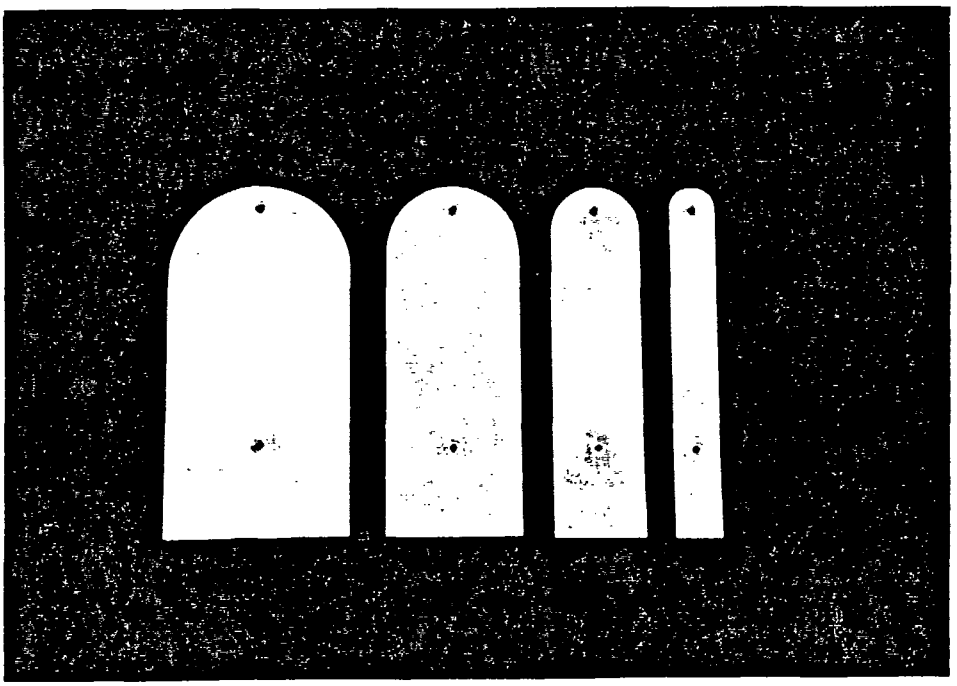

Figure 6: Endplate wing-tips (left to right: 4", 3", 2", 1")

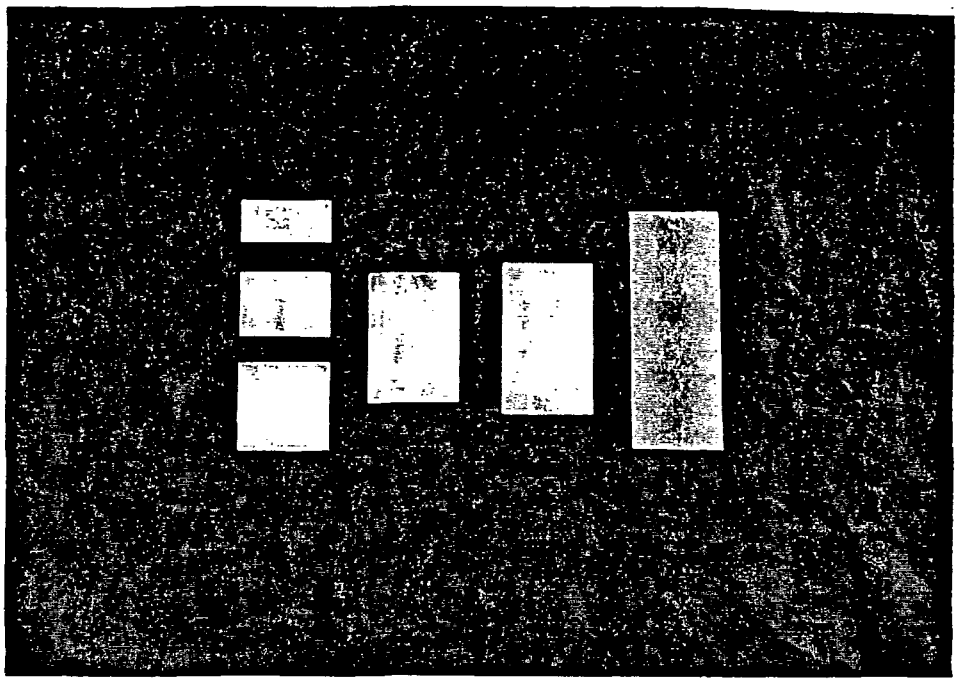

Figure 7: Subwing wing-tips (top to bottom, left to right: 0.5", 1", 1.5", 3")

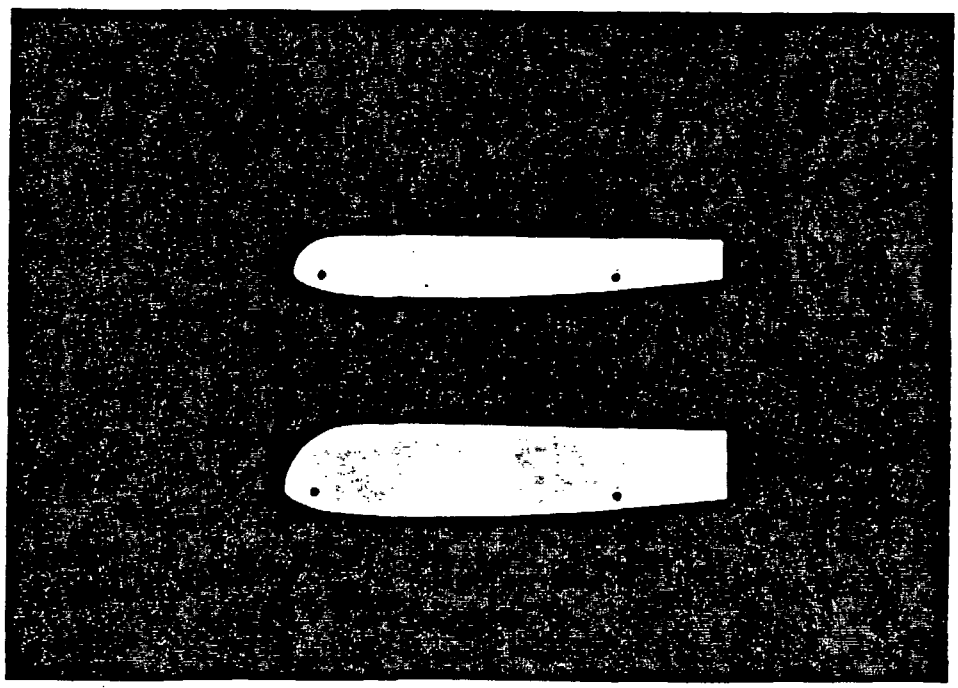

Figure 8: Half Endplate wing-tips (top to bottom: 0.75", 1.25")

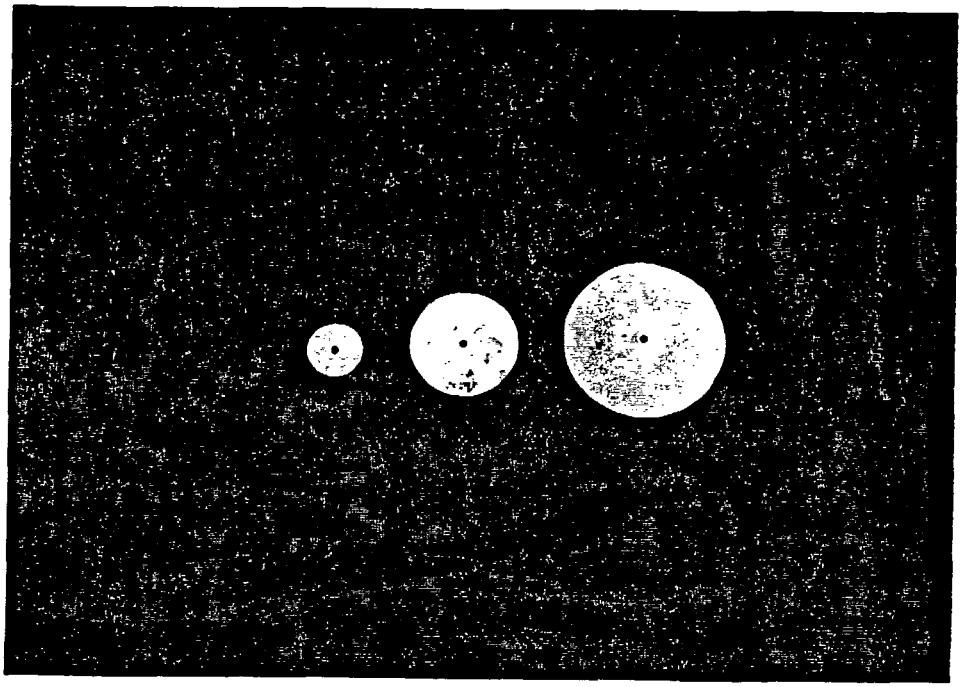

Figure 9: Circular Tip-Plate wing-tips (left to right: 1", 2", 3")

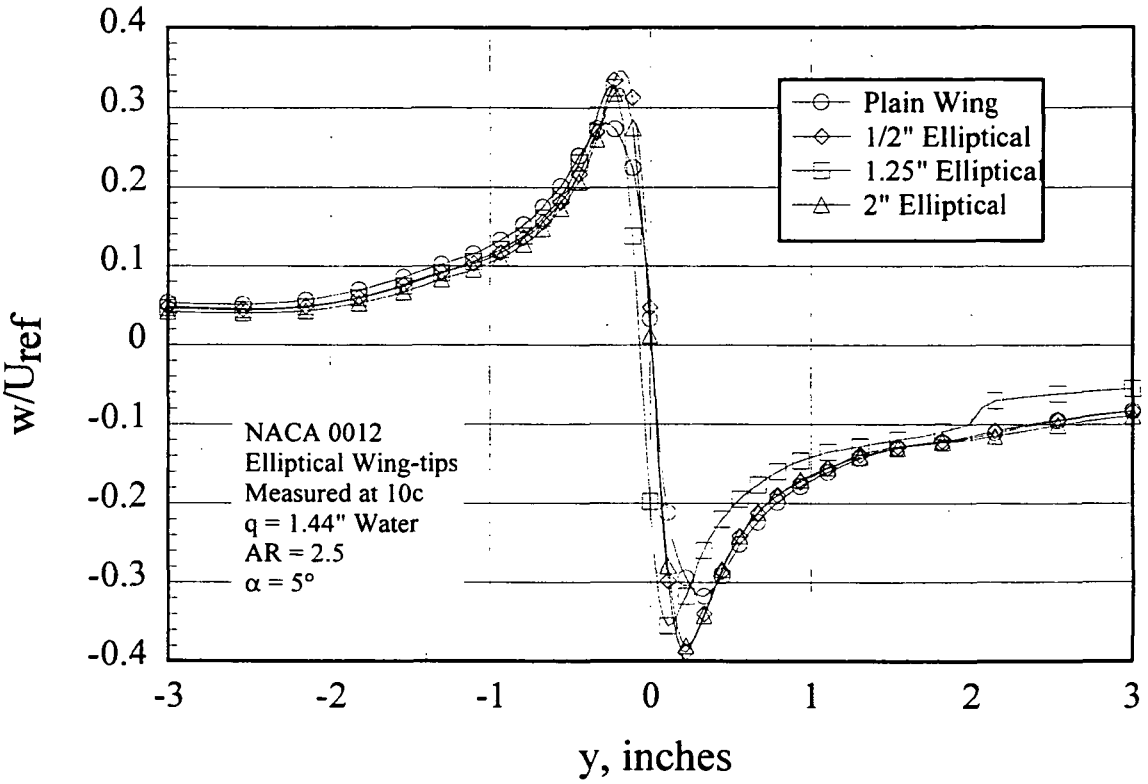


Figure 10: Velocity Profile of NACA 0012 airfoil section with variable size Elliptical Tips

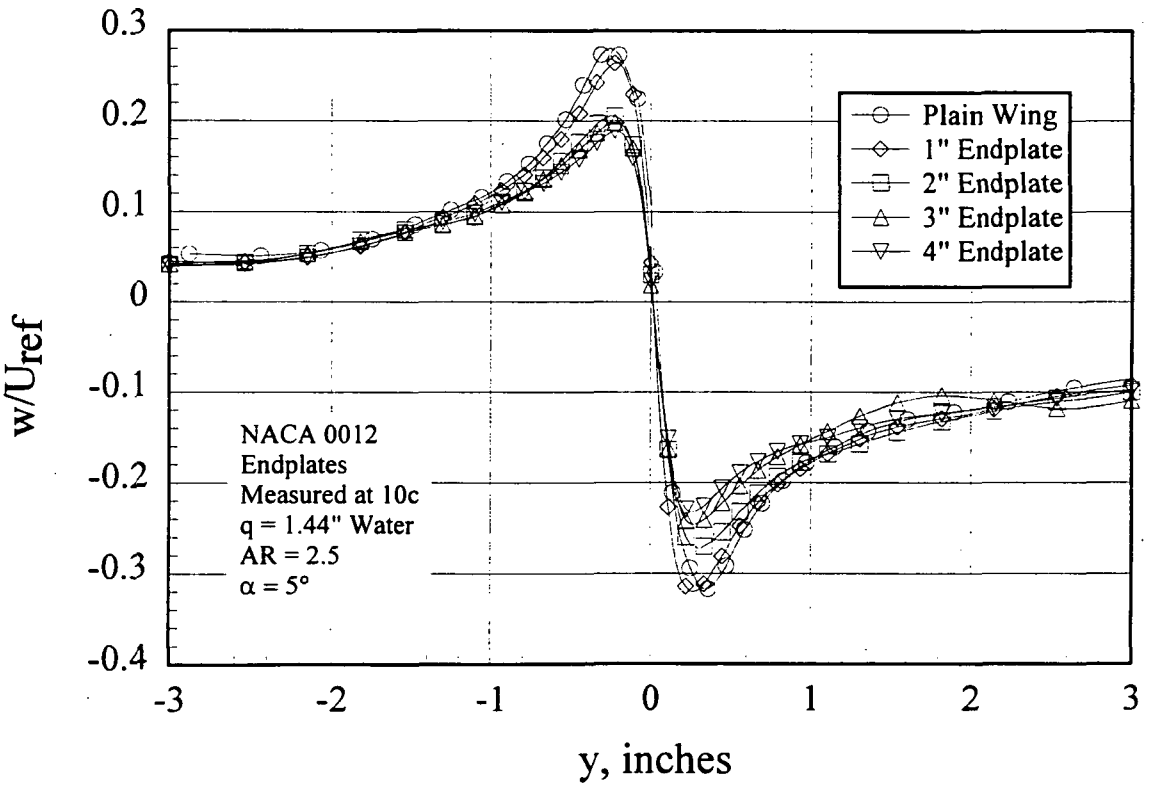


Figure 11: Velocity Profile of NACA 0012 airfoil section with variable size Endplates

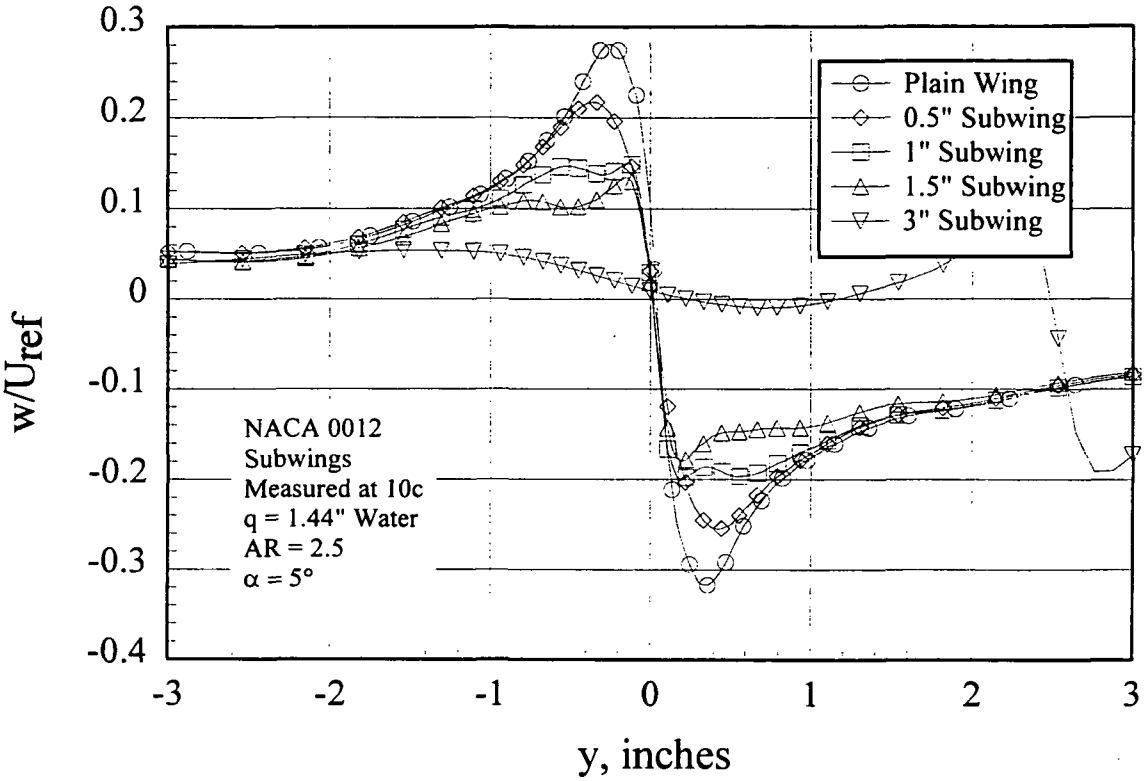


Figure 12: Velocity Profile of NACA 0012 airfoil section with variable size Subwings

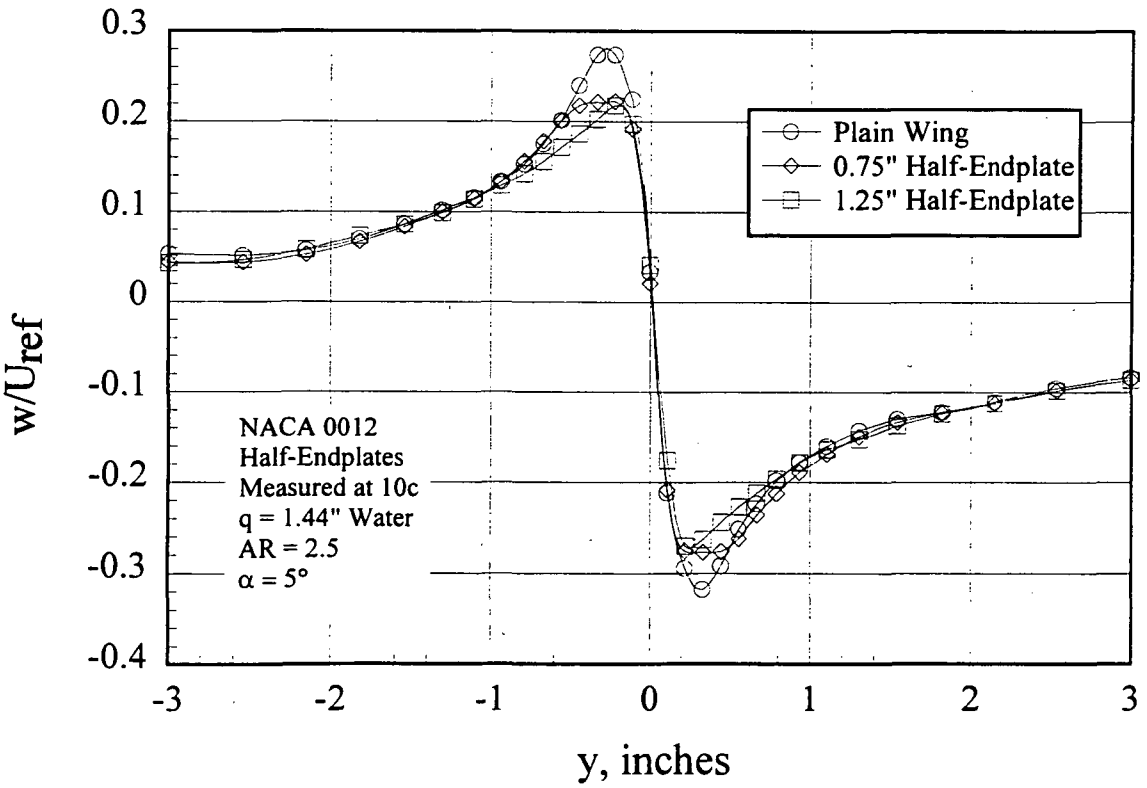


Figure 13: Velocity Profile of NACA 0012 airfoil section with variable size Half-Endplates

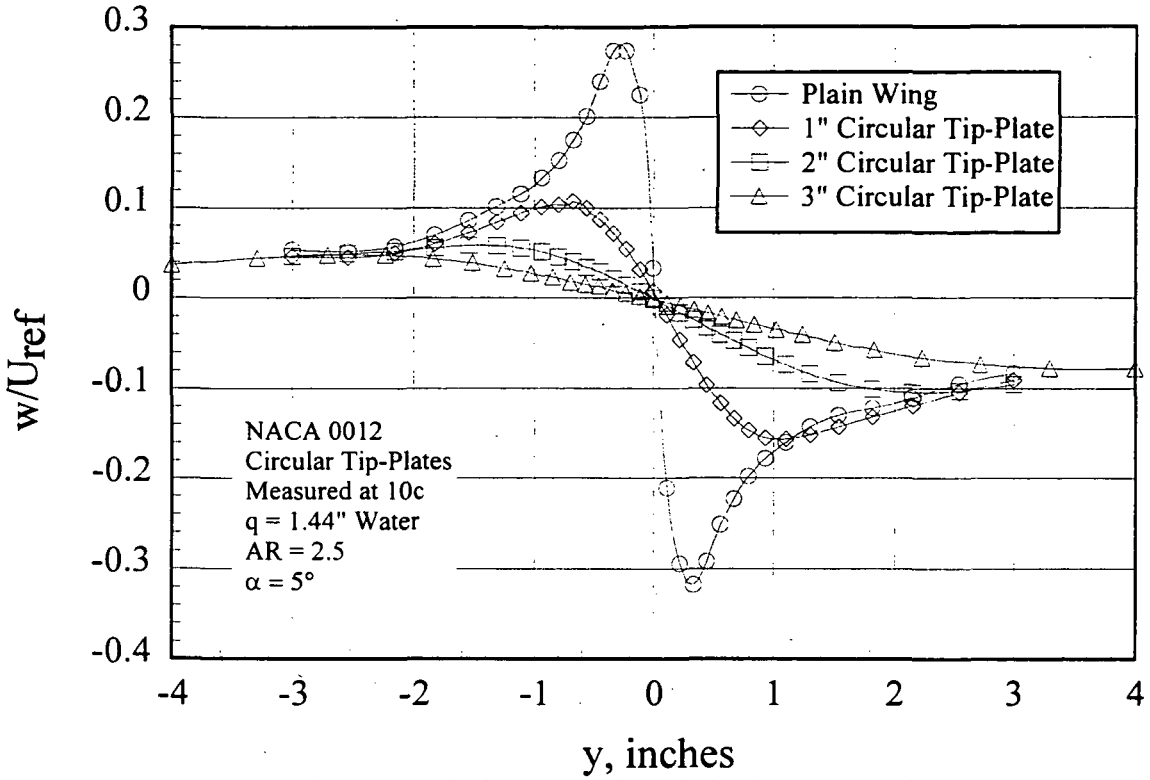


Figure 14: Velocity Profile of NACA 0012 airfoil section with variable size Circular Tip-plates

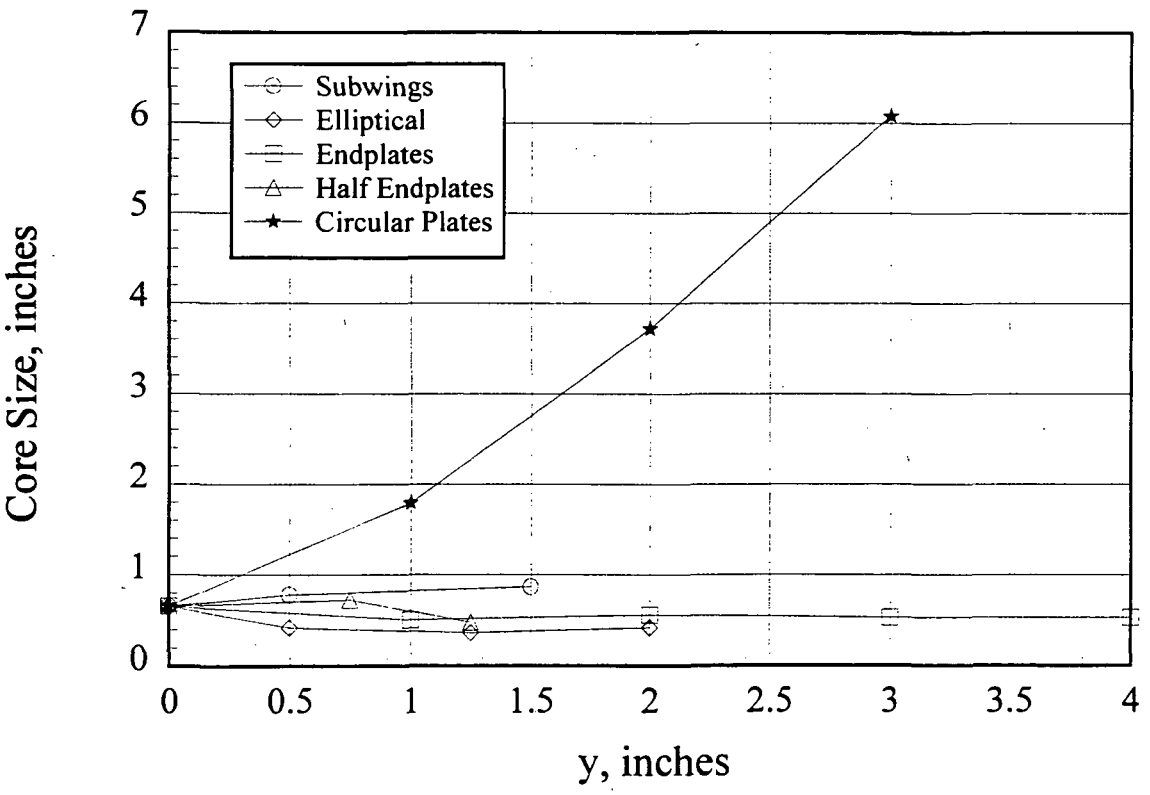


Figure 15: Trailing Tip Vortice Core Trend Sizes for Wing-tips Tested

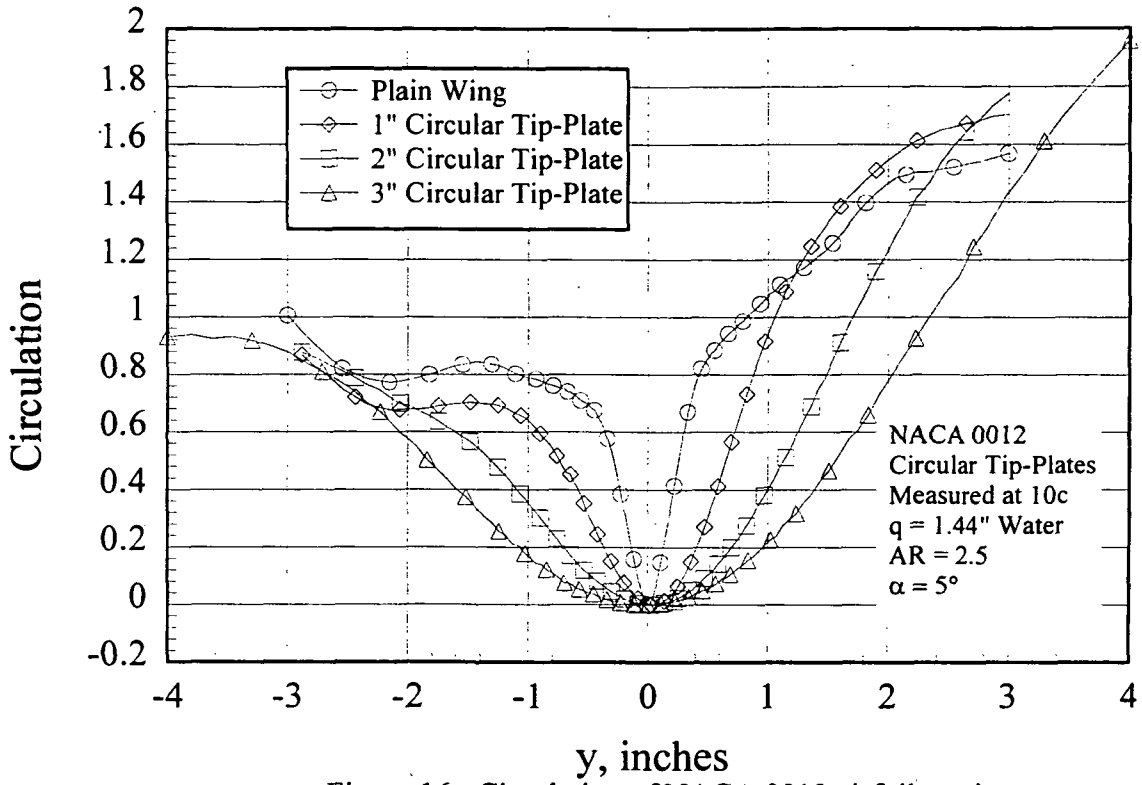


Figure 16: Circulation of NACA 0012 airfoil section with variable size Circular Tip-plates